AD-A049 334 NAVAL AIR PROPULSION CENTER TRENTON NJ PROPULSION TE--ETC F/G 11/8
EFFECTIVENESS OF THE REAL TIME FERROGRAPH AND OTHER OIL MONITOR--ETC(U)
NOV 77 D POPGOSHEV, R VALORI

UNCLASSIFIED NAPC-PE-2 NL

1 OF 1
AD A049334

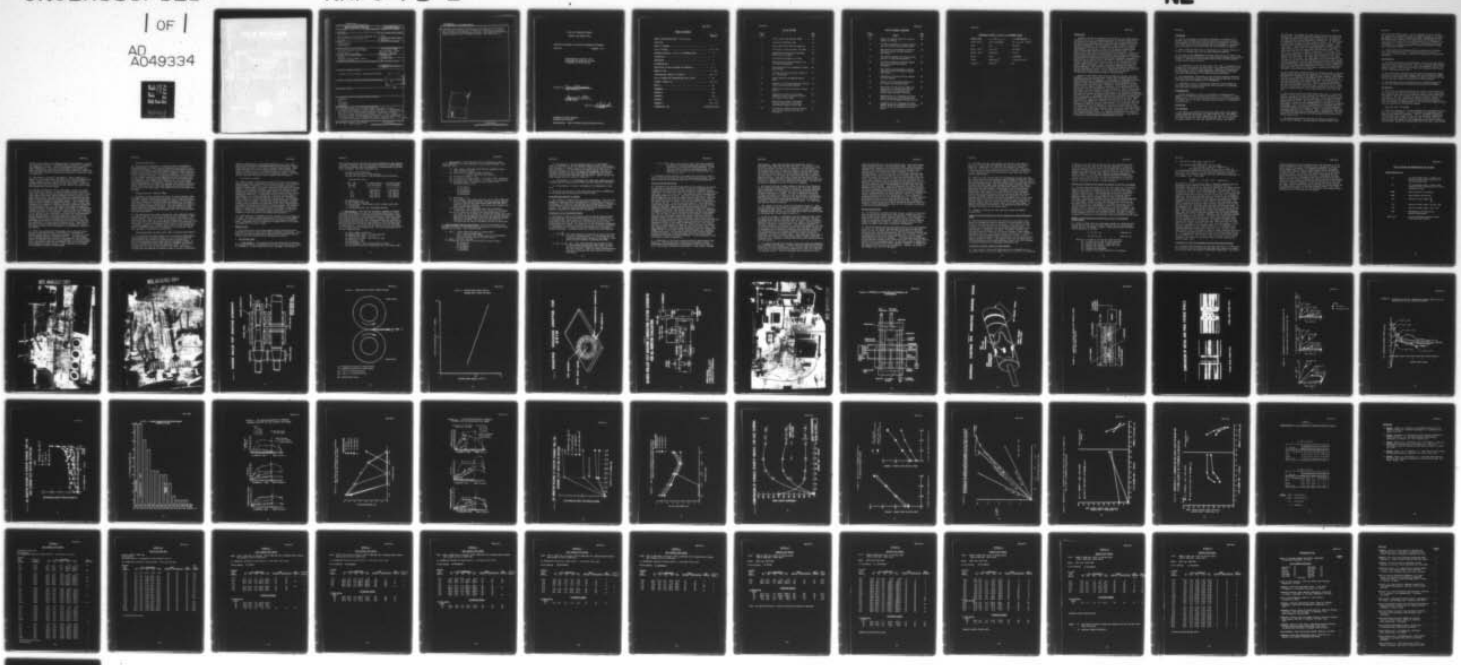

END
DATE FILMED
3-78
DDC

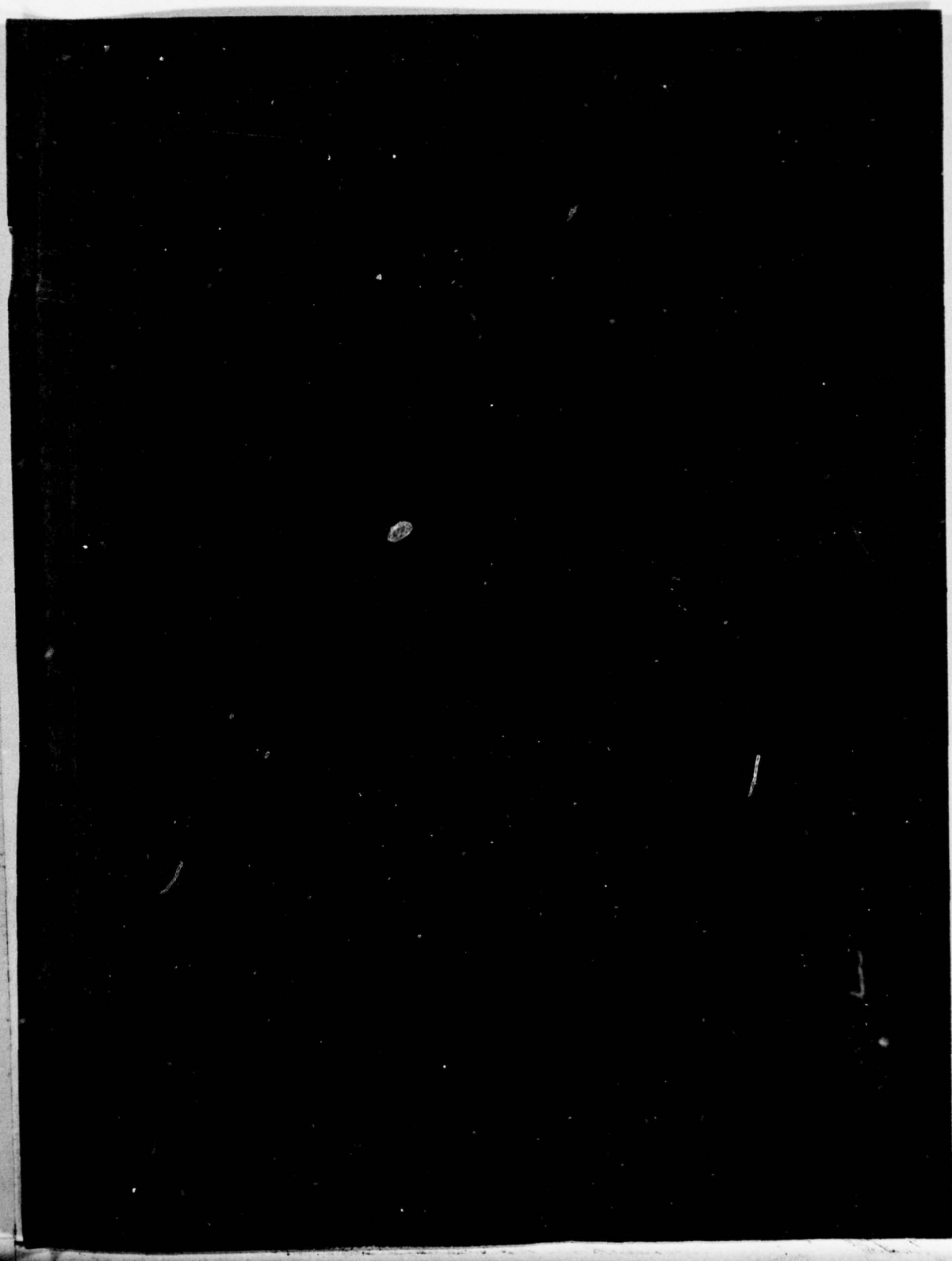

UNCLASSIFIED

SECURITY CLASSIFICATION OF THIS PAGE *(When Data Entered)*

REPORT DOCUMENTATION PAGE

READ INSTRUCTIONS BEFORE COMPLETING FORM

1. REPORT NUMBER: NAPC-PE-2
2. GOVT ACCESSION NO.:
3. RECIPIENT'S CATALOG NUMBER:

4. TITLE *(and Subtitle)*: Effectiveness of the Real Time Ferrograph and Other Oil Monitors as Related to Oil Filtration

5. TYPE OF REPORT & PERIOD COVERED: Phase

6. PERFORMING ORG. REPORT NUMBER: NAPC-PE-2

7. AUTHOR(s): Daniel Popgoshev; Raymond Valori

8. CONTRACT OR GRANT NUMBER(s):

9. PERFORMING ORGANIZATION NAME AND ADDRESS: Naval Air Propulsion Center (PE72), P.O. Box 7176, Trenton, New Jersey 08628

10. PROGRAM ELEMENT, PROJECT, TASK AREA & WORK UNIT NUMBERS: Program Element - 62241N; Task Area - WF 41-401; Work Unit - NAPC 877

11. CONTROLLING OFFICE NAME AND ADDRESS: Commander, Naval Air Systems Command, AIR-330, Washington, DC 20361

12. REPORT DATE: November 1977

13. NUMBER OF PAGES: 65

14. MONITORING AGENCY NAME & ADDRESS *(if different from Controlling Office)*:

15. SECURITY CLASS. *(of this report)*: Unclassified

15a. DECLASSIFICATION/DOWNGRADING SCHEDULE:

16. DISTRIBUTION STATEMENT *(of this Report)*: Approved for Public Release: Distribution Unlimited

17. DISTRIBUTION STATEMENT *(of the abstract entered in Block 20, if different from Report)*:

18. SUPPLEMENTARY NOTES:

19. KEY WORDS *(Continue on reverse side if necessary and identify by block number)*:
Ferrograph
Wear
Oil Analysis
Filtration
Diagnostics

20. ABSTRACT *(Continue on reverse side if necessary and identify by block number)*:
A development model of an oil monitor known as the Real Time (R.T.) Ferrograph was evaluated on a bench tester to determine its effectiveness in detecting rolling contact fatigue or scoring type failures, especially as influenced by various levels of oil filtration. Comparisons of the R.T. Ferrograph are made with spectrometric oil analysis, a light scattering and attenuation device, an X-ray fluorescence device, a particle counter, and the analytical Ferrograph. Results of the testing showed the R.T.

OVER

DD FORM 1 JAN 73 1473 EDITION OF 1 NOV 65 IS OBSOLETE S/N 0102-014-6601

UNCLASSIFIED

SECURITY CLASSIFICATION OF THIS PAGE *(When Data Entered)*

Ferrograph to be effective in detecting failures when the oil filtration level was above 40 micrometres. In addition, it correlates well with the other oil monitors at these filtration levels. Below the 40 micrometre oil filtration level the R.T. Ferrograph was found to be ineffective.

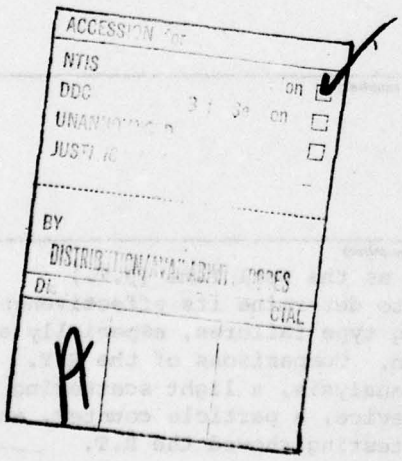

NAVAL AIR PROPULSION CENTER

TRENTON, NEW JERSEY 08628

PROPULSION TECHNOLOGY AND PROJECT ENGINEERING DEPARTMENT

NAPC-PE-2

NOVEMBER 1977

EFFECTIVENESS OF THE REAL TIME FERROGRAPH AND OTHER OIL MONITORS AS RELATED TO OIL FILTRATION

Prepared by: Daniel Popgoshev
DANIEL POPGOSHEV

Raymond Valori
RAYMOND VALORI

Approved by: A. Lockwood
A. LOCKWOOD

AUTHORIZATION: NAVAIR AIRTASK AO3P0000/052B/6F41-432-301

TABLE OF CONTENTS

LIST OF FIGURES

LIST OF FIGURES (CONTINUED)

CONVERSION FACTORS: SI TO U. S. CUSTOMARY UNITS

Convert from	To	Multiply By
degree Kelvin	degree Fahrenheit	$t_F = t_K (1.8) - 459.67$
metre	inch	39.370079
metre $-sec^{-1}$	inch sec^{-1}	39.370079
$metre^2 -sec^{-1}$	centistoke	1×10^6
Newton	pound	0.22480894
Pascal	$pound\text{-}inch^{-2}$	$1.45037743 \times 10^{-4}$
$rev\text{-}sec^{-1}$	$rev\text{-}min^{-1}$	60

INTRODUCTION

Diagnostic methods for determining the health of gas turbine engines include the use of oil contamination monitors as important indicators of the condition of lubricant wetted components such as gears and bearings. Two devices used extensively are (a) in-line chip detectors and (b) the emission spectrometer. The chip detector is used to detect a rapidly progressing failure before it becomes catastrophic while the emission spectrometer is used as part of the Joint Oil Analysis Program (JOAP) which involves monitoring and trending contamination levels. The magnetic wear debris which normally actuate a chip detector are generally large particulates above 200 micrometres in major dimension (reference 1) while emission spectrometric analysis (SOA) has been shown to be effective in detecting very small particles below eight micrometres (reference 2). Data from SOA is normally used in the JOAP for tracking the health of an engine or component by observing the change in the concentration levels of many elements with time. Using this time scaled trending technique, JOAP has had considerable success in detecting impending failures in engine components. The failures are generally indicated by increases in the iron concentration level. This is consistent with the fact that most critical load bearing surfaces in gas turbine engine gearboxes and helicopter transmissions are made of hardened steels.

There is a large range (above eight micrometres and below 200 micro-micrometres) of wear particle sizes in which chip detectors and SOA are generally ineffective (reference 2). Also, there is considerable evidence that abnormally wearing components are detectable by measuring, with respect to time, the amount and variations in size distribution of wear particles within this size range. Therefore, a need exists to develop a device which is capable of detecting failures, in a timely manner, by observing particle size distributions and contamination levels in this range. Accordingly, the Navy initiated a program in FY72 to develop an airborne real time version of a laboratory device known as the Analytical Ferrograph. This device is capable of separating microscopic size magnetic wear particles according to size. A development model of one unit known as the Real Time (R.T.) Ferrograph was delivered to the Naval Air Propulsion Center (NAPC) for evaluation. Reference 3 describes the functions of the unit. The purpose of this report is to document the evaluation of the unit with respect to oil filtration level on a bench tester. Oil filtration level was considered an important parameter for defining the applicability of the R.T. Ferrograph, since oil filtration level varies widely from one engine to another. For comparative purposes, other oil monitors were also used in the same system and included: (a) an X-ray fluorescence unit, (b) a light scattering/attenuation device, (c) emission spectrometric oil analysis, (d) a particle counter, and (e) the Analytical Ferrograph. This work was authorized by NAVAIR AIRTASK AO3P0000/052B/6F41-432-301.

CONCLUSIONS

1. The R.T. Ferrograph, as presently configured, is effective in detecting rolling element bearing fatigue and disc scoring type failures if the nominal oil filtration level is above 40 micrometres. At filtration levels finer than 40 micrometres, the R.T. Ferrograph is ineffective. At the 40 micrometre filtration level, its effectiveness is marginal.

2. Under conditions when the R.T. Ferrograph is an effective failure detector, it correlates well with the other diagnostic methods.

3. The ratio of the concentration of small wear particles to that of the large wear particles has proven to be a poor index or measure of the severity of wear. A function of the difference between large and small particle concentrations is more effective.

4. The sensitivity of the Severity Index, $(A_L^2 - A_S^2)$, is affected by the volume of oil flow through the system and by the differences in the rates of generation of large and small particles. Therefore, in applying the R.T. Ferrograph, the oil volume sampled should be matched to the wear generating characteristics of the machinery being monitored.

5. The preponderence (99 percent) of wear particle generation resulting from disc scoring and rolling element bearing fatigue spalling is in the size range from two micrometres to 25 micrometres.

6. Comparison of the oil contamination diagnostic methods shows the bench-type light scattering/attenuation method and SOA to be effective over the widest filtration range.

RECOMMENDATIONS

Further development of the R.T. Ferrograph is recommended with emphasis on incorporating features which allow for a variable oil volume sampling rate. In this manner the sensitivity of the R.T. Ferrograph may be adjusted to suit the wear generating characteristics of the equipment being monitored.

DESCRIPTION

Test Equipment

1. All testing was conducted utilizing the Geared Roller Test Machine (GRTM), Mechanical Technology, Inc. (MTI) Model No. 201. The GRTM is designed such that the outside diameters of two test rollers in contact are loaded against each other and are operated, each at a different peripheral velocity, so that both sliding and rolling take place at

the same time. The amount of sliding and rolling can be varied over a wide range. An overall view and a close-up of the test section of the GRTM are shown in Figures 1 and 2, respectively. In addition, the test section is shown schematically in Figure 3. The test rollers are mounted on two parallel shafts (refer to Figure 3) on a 0.0762m (3 inch) center distance and the shafts are geared together. Each test roller is 0.0762m (3 inch) in diameter with a 0.3556m (14 inch) crown radius. Power input is through the lower shaft, the upper shaft being driven by the lower shaft through phasing gears. These gears may be any one of a number of ratios (1.0, 1.07, 1.14, 1.22, 1.50, 1.73, 2.0 or 3.5) to produce a wide range of controlled sliding and rolling velocities at the contact point depending on the input speed of the lower shaft. The lower shaft is electric motor driven through a set of pulleys. The shaft speed can be varied from 8.1 rps (485 rpm) to 105 rps (6300 rpm) depending on the pulley ratio selected. A given combination of pulley ratio and phasing gear ratio represents one operating point. Each operating point may be used to closely simulate the rolling/sliding conditions which occur at one point along the actual tooth profile of a gear (Note: sliding and rolling vary from point to point on a gear tooth).

2. The rolling and sliding velocities are defined as shown in Figure 4. Figure 4 shows that the rolling velocity, V_R, is defined as the sum of the tangential velocities of the upper and lower rollers. The sliding velocity, V_S, is defined as the absolute value of the difference of these two velocities. The slide-to-roll ratio is defined as the sliding velocity divided by the rolling velocity. Pure rolling exists when the sliding velocity is zero. A set of special elliptical phasing gears were available whose gear ratio varied from 0 to 1.5. With the use of these gears, the test rollers experienced varying rolling/sliding conditions similar to those experienced by a gear tooth contact.

3. The two test rollers are loaded against each other in "nutcracker" fashion. The upper and lower frames of the machine (see Figure 1) are fastened together at one end by a hinge pin. For operation, the upper frame is pivoted downward to bring the rollers into contact and the phasing gears into mesh. The load is applied to the free end of the upper frame through a lever arrangement which is actuated by a pneumatic rotochamber. The actual load is determined by a calibrated load cell. The maximum contact or Hertz stress that the test rollers experience varies with applied load as shown in Figure 5. The housing serves as a controlled temperature oil reservoir. Heat is provided by a 2000 watt - 115V immersion heater which is controlled by a thermoswitch. The test rollers are jet lubricated with the jet directed at the outlet of the roller contact area.

4. The GRTM was modified to allow for the testing of bearings in rolling contact fatigue. The modification involved removal of the

upper shaft and phasing gears. The test specimen on the lower shaft was replaced by a bearing and housing as shown in Figure 6. An adapter was mounted on the shaft to achieve the proper interference fit with the bearing bore. Rotation of the bearing O.D. was prevented by the use of set screws which fit into small ground holes on the bearing O.D. (See Figure 6). A radial load is applied to the bearing housing and transmitted to the bearing by means of the same "nutcracker" arrangement previously described.

5. A displacement type vibration pick-up is mounted on the loading arm. This instrument acts as a failure sensor and can be set to terminate the test on either a test roller or bearing at various stages of failure.

Test Materials

6. The test rollers used on the GRTM during the series of disc scoring tests were made of SAE 4720H steel. This is a carburized case hardened steel with a case hardness of 62 R_c and a core hardness of 40 R_c. The surface roughness of the rollers is 0.46-0.56 micrometres (18-22 micro-inches) centerline average (CLA).

7. The test bearings used were SKF type NJ212 roller bearings (double flanged outer ring, and single flanged inner ring) modified, by removing eight of the sixteen roller elements, in order to decrease the load capacity and life, thereby accelerating the bearing failure.

8. The lubricant used in the system was an oil qualified under the aircraft gas turbine engine lubricant specification MIL-L-23699B.

Oil Monitors

9. Two of the oil monitors used during the course of this program, the R.T. Ferrograph and the United Technologies Research Center X-ray Wear Metal Monitor, were placed in the GRTM oil system as shown schematically in Figure 7. The R.T. Ferrograph, as shown in Figure 8, had its own recirculating oil loop. Bench style lubricant condition monitors (SOA, Analytical Ferrograph and light scattering/attenuation device) were also utilized to analyze samples of the oil from the GRTM oil system. These oil monitors are described as follows:

Real Time (R.T.) Ferrograph

10. The R.T. Ferrograph is an engine mountable device designed to operate in a test cell environment. It is a variation of a laboratory device known as the Analytical Ferrograph. The R.T. Ferrograph functions by precipitating, from a sample of oil, iron wear particles continuously along a glass tube according to particle size. Readings, which are dependent upon the amount of light transmittance, are taken at both the small particle end and the large particle end of the tube. Both readings

are felt to be necessary to determine trends in wear behavior. Details of the operation of the R.T. Ferrograph are as described in reference 3 and summarized as follows. The R.T. Ferrograph system consists of three assemblies;i.e. the Real Time Ferrograph, (Trans-Sonics Type 7081), the Pump Unit (Type 7083), and the Control/Indicator (Type 7082). This particular system was developed for mounting on an engine oil tank in a test cell.

11. The operation of the R.T. Ferrograph is shown schematically in Figure 9. Oil is drawn from a reservoir or oil tank and pumped to the inlet. From there the oil travels through the precipitator tube, through a sample reservoir and out the oil return line. A vent line from the unit to the oil reservoir or tank relieves the system of any flow reversal once the pump stops.

12. The optical system of the R.T. Ferrograph consists of a series of six fiber optic bundles. A light is passed through three of the fiber optic bundles and focused through the precipitator tube to three other fiber optic bundles directly opposite and then carried to the photo resistor bank. The fiber optic bundles are positioned at three points along the precipitator tube and the tube itself is positioned within a highly divergent field gradient magnet. The reference fiber optic is placed outside the magnetic field and is used to adjust lamp voltage so as to maintain a constant electrical resistance through the sensing photoresistors; i.e. this adjusts the voltage to negate any oil color effects. The other two fiber optic bundles are focused downstream in the tube in areas where large (greater than two micrometres) and small particles are precipitated. These particles cause a decrease in the intensity of the light which is proportional to the percentage area of the tube which is covered by particles. The readout is a digital representation of the percentage area covered at each precipitation station and is displayed on the Control/Indicator. The percentage area covered at the large particle location is symbolized by A_L and that of the small particle location by A_S. These two outputs can be used in several ways for failure analysis and trending, the details of which will be discussed in the "Discussion" section of this report.

13. Within the precipitator tube housing, the oil flows by gravity feed to the precipitator tube. The overall R.T. Ferrograph oil sampling system recycles automatically whenever all of the oil in the R.T. Ferrograph reservoir has drained out and an air bubble passes across the reference photo resistor. This change in light intensity causes a pulse which shuts off the electromagnet and recycles the pump unit. This process cleans the precipitator tube of any particulates and recharges the system reservoir. After operating in this manner for 30 seconds the sensor is reactivated.

Analytical Ferrograph

14. The Analytical Ferrograph is a laboratory device, developed by Foxboro/Trans-Sonics, which is used to precipitate wear particles contained in an oil sample. The wear particles are precipitated according to size on a specially coated glass slide by means of a highly divergent magnetic field similar to that of the R.T. Ferrograph. This resulting slide is called a Ferrogram. A microscopic examination of the Ferrogram is used to help determine the wear mechanism by which the particulates were generated. This examination reveals the nature of the particles; e.g. material type and type of wear (reference 4). The most heavily precipitated portion of a Ferrogram is the area where the oil sample begins to deposit onto the slide. An analysis of the density and height of this "entry area" shows that these variables are closely related to the severity of the wear regime of the system from which the sample was obtained.

General Electric Oil Monitor (GEOM)

15. The GEOM is a bench mounted device which is used to analyze a small oil sample (usually 20 milliliters) by means of the scatter and attenuation of a beam of light passing through the sample. The light scattering output is related to the particulate concentrations in the sample while the attenuation is related to the color and degradation of the oil. Figure 10 shows a diagram of the sensor. The light source is a beam of highly concentrated infrared radiation. Directly opposite the light source (180°) is the attenuation photodiode, and at 90° from the source the scatter photodiode.

16. The GEOM outputs are scatter, attenuation, and a reference calibration check. They are read on a dial meter and are controlled by a meter selector switch. Prior to operation of the system a calibration is required with clean unused oil of the type being monitored. This calibration is set by zero and span potentiometers, located inside the rear of the control box. To operate the monitor an oil sample is either poured into the sensor assembly or the assembly placed in an oil tank, and the test button is depressed after which the reading for the particular channel being observed is indicated on the meter dial.

United Technologies Research Center (UTRC) X-ray Wear Metal Monitor

17. The UTRC X-ray Wear Metal Monitor is an in-line X-ray fluorescence system and operates as shown in Figure 11. As oil flows through the sensor chamber, two radioactive isotope sources (plutonium 238; 30 millicuries) irradiate it with X-rays through transparent windows. As the oil is bombarded by these X-rays there is a movement of electrons from the inner (K) shell of the iron atom which causes a shift in electrons from the outer shells to fill in the voids. This motion is accompanied by the emission of secondary X-rays or photons (fluorescence)

which are characteristic of the excited material, e.g. iron. This activity is sensed by an argon/methane gas filled proportional counter which yields an output in the form of millivolt analog pulses. These pulses are then put through a signal processer, which contains the logic and gating circuitry to convert the pulses to digital form for analysis of concentration of the iron in parts per million. Additional details concerning this device can be obtained from reference 5.

Royco Particle Counter

18. A Royco Particle Counter was also used during this test program to determine the number of particles in a specific volume of oil following various degrees of filtration. The Royco Instruments, Liquidborne particle counter, Model 345 (counter), Model 342 (adsorption and scatter sensor) is a laboratory instrument. This instrument gauges the size of particles going through a 400 micrometre sample cell by means of the scatter and attenuation of a very sharply defined beam of light focused through the sample cell. A photodiode is used as the light sensor on each channel. As a particle passes the light beam, the photodiodes sense a reduction in light and generate a signal pulse. The amplitude of this pulse is related to particle size while the duration is proportional to particle length. The particle counter then takes a running average of the concentration of particles in the various predetermined size ranges and displays the output on a digital screen. The system is sensitive to particles from two micrometres in diameter to 400 micrometres in diameter in concentrations up to 100,000 per 100 cubic centimetres. An internal calibration allows the detection circuit to correct for color variations in the sample being analyzed.

19. Sample analysis is performed by first subjecting the test sample to a vacuum. This process reduces the quantity of air in the test sample; i.e., air will cause erroneous readings since the bubbles can deflect light. Afterwards the oil is poured into a sample holder on the sensor and pumped past the optical system.

METHOD OF TEST

1. Disc scoring tests and rolling element bearing fatigue tests were conducted in order to simulate both gear and bearing type failures. Three series of disc scoring tests and one series of rolling element bearing fatigue tests were conducted and are described as follows:

2. Disc Scoring Tests

a. Test Series 1: The purpose of this test series was to determine the response of the R.T. Ferrograph with time by using slide-to-roll ratio as a parameter. As the slide-to-roll ratio increases, the severity of

wear increases and the wear particle size distribution is also expected to change. Therefore, the R.T. Ferrograph's ability to reflect differences in wear particle size distributions and the magnitude of the wear can be evaluated. The test conditions were:

(1) Load - 4741 N (1066 lbs)
(2) Max. Hertz Stress 1.73 GPa (248 KSI)
(3) One test run at each of the following speed conditions:

Slide-to-roll ratio $\frac{\lvert V_A - V_B \rvert}{V_A + V_B}$	V_A (lower roller), m/s (inch/sec)	V_B (upper roller), m/s (inch/sec)
0	3.49 (137.4)	3.49 (137.4)
0.1	3.49 (137.4)	4.25 (167.5)
0.2	3.49 (137.4)	5.27 (207.5)
0.27	3.49 (137.4)	5.91 (232.5)
0.33	3.49 (137.4)	7.05 (277.6)

(4) Lubrication - jet
(5) No filtration was used
(6) Test duration: Four hours or until scoring, which ever occurs first
(7) Oil monitors used: R.T. Ferrograph and SOA

b. Test Series 2: This test was originally intended to evaluate the effect of filtration on the R.T. Ferrograph effectiveness using elliptical drive gears so that the test disc would experience a varying slide-to-roll ratio. This varying slide-to-roll ratio was intended to closely simulate gear tooth action. However, only a baseline test using no filtration was run. Continued testing was cancelled because the baseline test was too time consuming. The filtration tests were then run using a constant slide-to-roll ratio and are described in "Test Series 3". The results of the baseline test for Test Series 2 are of interest and are reported herein. The test conditions for the one test conducted were:

(1) Load - 26980 N (6066 lbs)
(2) Maximum Hertz Stress - 3.05 GPa (442 KSI)
(3) Slide-to-roll ratio - 0.0 to 0.2
(4) Speed of drive gear - 91.6 rps (875 rpm)
(5) Filtration - none
(6) Lubrication - jet
(7) Test duration - until scoring failure occured
(8) Oil Monitors used; R.T. Ferrograph, SOA, UTRC X-ray, GEOM

c. Test Series 3: This test series was to determine the effect of oil filtration on the detectability of scoring type failures. Test conditions were:

(1) Load - 4741 N (1066 lbs) until failure; reduced to 2518 N (566 lbs) after failure
(2) Hertz Stress 1.73 GPa (248 KSI) to failure
1.38 GPa (201 KSI) after failure
(3) Slide-to-roll ratio - 0.33
(4) V_B (Velocity of upper roller) = 7.05 m/sec (277.6 inches/sec)
(5) V_A (Velocity of lower roller) = 3.49 m/sec (137.4 inches/sec)
(6) Filtration level: one test was run at each of the following nominal levels:

No filtration
75 micrometres
40 micrometres
25 micrometres
10 micrometres

(7) Lubrication - jet
(8) Test duration - The roller discs were run at 4741 N (1066 lbs) until a scoring failure occurred. The load was then reduced to 2518 N (566 lbs) for five minutes after which the 4741 N (1066 lb) load was reapplied. This process was followed until three scoring events occurred.
(9) Oil Monitors: R.T. Ferrograph, SOA, GEOM, and during selected tests Royco Particle Counter, Analytical Ferrograph
(10) At the completion of each of the scoring tests the oil in the system was recirculated for five minutes through each successively finer filter than that with which the test was conducted. Readings on the applicable oil monitors were obtained at each filtration increment. This series is referred to as a "recirculating oil series" throughout the text of this report.

3. Rolling Element Bearing Fatigue Tests: This test series was run to determine the effect of filtration on the detectability of bearing contact fatigue type failures. Test conditions were:

a. Load - 18085 N (4066 lbs) prior to fatigue spall
- 4741 N (566 lbs) after spall
- Note: generation of a fatigue spall was accelerated by etching the inner race of the test bearing.
b. Speed - 549.8 rps (520 rpm)
c. One test was run at each of the nominal filtration levels
No filtration
75 micrometre
40 micrometre
25 micrometre
10 micrometre

d. Test duration - The test bearings were run at the 18085 N (4066 lb) load until an initial spalling failure occurred. Testing was then continued at a reduced load of 4741 N (566 lbs) in order to avoid excessive vibration. The test bearing was examined every four hours to determine the extent to which the damage had propagated. The test was terminated whenever the spall had progressed halfway around the inner raceway or until machine vibrations were excessive. Typical initial and final fatigue spalls are shown in Figure 12.

e. Oil Monitors: R.T. Ferrograph, SOA, UTRC X-ray, GEOM and during selected tests the Royco Particle Counter and the Analytical Ferrograph.

f. Recirculating oil series - performed at the completion of each test.

4. During the entire phase of each test series the bulk oil temperature in the system sump was maintained at 310.9°C (100°F).

DISCUSSION AND ANALYSIS OF RESULTS

1. This section is divided into eight major sub-headings. The first sub-heading is concerned with the interpretation of the outputs of the R.T. Ferrograph. The second two sub-headings are concerned with the discussion of the results of the test series as described in the "Method of Test" section. The remaining major sub-headings discuss and analyze various aspects of the data for comparison and correlation.

Discussion of R.T. Ferrograph Outputs

2. The outputs of the R.T. Ferrograph unit are digital representations of the percentage area covered with particles at two locations on the precipitator tube. These outputs are denoted as A_L for percentage large area covered (particles greater than 2 micrometres), and A_S for percentage small area covered. For simplicity in the monitoring of machinery it is desirable to combine the outputs (A_L and A_S) of the R.T. Ferrograph in some manner into one index which will be indicative of the wear or failure in progress. Currently, three such indices have been suggested:

a. $SI_1 = \frac{A_L}{A_S}$; This index indicates the severity of wear as the ratio of large to small particles. It was thought that the sudden disproportionate increase in the number of large particles would indicate an abnormal wear mode.

b. $SI_2 = A_L (A_L - A_S)$; This index indicates the severity of wear as the difference between the output values of large and small particles weighted by the output value of the large particles. Again any sudden disproportionate increase in large particle count indicates a severe wear regime.

c. $SI_3 = (A_L^2 - A_S^2) = (A_L + A_S)(A_L - A_S)$; This index indicates the severity of wear as weighted by both the sum and difference of the particle size distribution. It may also be viewed as SI_2 plus a weighting factor for variations in the small particle distributions, i.e. $SI_2 + A_S (A_L - A_S)$.

3. A majority of the figures in this report are presented in terms of SI_2 as it was preferred at the time the figures were prepared. SI_3 has since evolved as the preferred index due to its greater sensitivity.

The Disc Scoring Test Series

4. As stated in the "Method of Test Section" the purpose of this series of tests was to determine the ability of the R.T. Ferrograph to distinguish among various levels of wear and different particle size distributions. Five tests were run each at different levels of slide-to-roll ratio (0.0, 0.1, 0.2, 0.27, 0.33). The severity of wear increases with increasing slide-to-roll ratio. This test series was run at a load of 4741 N (1066 lbs). No filter was used in any of these tests. Each test was run either for four hours or until scoring occurred on the discs. The results are shown in Figure 13 for the two Severity Indices SI_2 and SI_3 and for the SOA. It can be seen that there is a clear and direct relationship between the R.T. Ferrograph response and the wear severity levels. In the three cases where no failures occurred the R.T. Ferrograph readings increased slightly and then leveled off indicating a normal-wear condition. The initial increase in output is a reflection of break-in wear during which the surface asperities are being sheared off. The two cases in which a failure occurred showed a continuously increasing R.T. Ferrograph output with time as reflected by the two severity indices and SOA. The R.T. Ferrograph output and the rate of increase of this output was higher for the more severe operating conditions. The R.T. Ferrograph severity indices also correlated well with the concentrations of iron in the system as determined by SOA. The severity index SI_1 is shown plotted in figure 14. Unlike the other two indices, SI_1 shows no clear trends with time and with slide-to-roll ratio. However, examination of figure 14 shows that after a period of running (for example at the 1.5 hour mark) the SI_1 index decreases with increasing slide-to-roll ratio. One can infer from this that the small particles are being generated at a proportionately higher rate than the large particles as the severity of wear increases. The data generated in this test series is given in Appendix A.

5. A second type of test was run using elliptical phasing gears (Test Series 2). The test discs were subjected to sinusoidally varying accelerations and decelerations with a maximum slide-to-roll ratio of 0.20. This phasing simulates the operation of a gear under a constant

load (stress). Data from this test were obtained for the R.T. Ferrograph, SOA, GEOM, and the UTRC X-ray unit. The outputs of these units are plotted, in Figure 15, for comparison in effectiveness. As can be seen, all of the oil monitors reacted in the same manner by increasing slowly during the test and rapidly as failure was reached. The increase in the outputs of the oil monitors was high as scoring failure occurred for all except the GEOM which exhibited a relatively shallow increase. (Only the scatter channel data was used for the GEOM since a linear regression analysis showed a correlation coefficient of 0.99 on a comparison of the scatter and attenuation). The data are presented in Appendix B for the oil monitors concerned.

6. The trend in aircraft turbine engines is towards finer filtration in the lubrication system as shown in Figure 16. This also indicates that the operating environment of an oil monitoring failure detection device will vary, i.e. the number and size of particulates will be different from engine to engine. In order to determine the effects of finer filtration on the ability of the oil monitors to detect an abnormal wear situation, a series of disc scoring tests were performed with steel mesh filters having nominal ratings of 10, 25, 40 and 75 micrometres installed in the GRTM lubrication system. One additional test was run without filtration.

7. The results of the test series are presented in Figure 17. Each test was normalized with respect to running time for ease of comparison in identifying wear trends. A "recirculating oil series" as described in "Method of Test" section was run at the end of each test and is shown in the second half of each graph in Figure 17.

8. At the "no filter", 75 micrometre, and 40 micrometre filter levels the GEOM and SOA showed an abnormal (high) wear condition. The R.T. Ferrograph shows similar trends with the "no filter" and 75 micrometre conditions but at the 40 micrometre level it shows an initial increase and then a decrease in severity level. This suggests that while an initially significant concentration of particles was generated, the rate of filtration was greater than the rate of wear generation. During the 25 micrometre and 10 micrometre filtration tests the GEOM, SOA and the R.T. Ferrograph (SI_2) show gradual increases but these are rather insignificant considering the magnitudes of the outputs of these oil monitors at the other filtration levels. These data would again tend to prove that the filtration rate was greater than or equal to the wear generation rate. Appendix C contains the detailed data generated during this test series.

9. Oil samples obtained from the sump of the test system were submitted for a particle count analysis. Figure 18 shows the wear particle distribution for the disc scoring series. All of these counts are normalized with respect to clean unused MIL-L-23699B from the same lot as was used for this test series. Figure 18 indicates that the majority of wear

particles generated are in the 2-10 micron range. The second largest group of particles are in the 10-25 micron range. These two groups taken together constitute over 99 percent of all particles generated. Therefore, the overwhelming majority of particles generated from a scoring type of wear process are below 25 microns in size. An apparant anomaly in Figure 18 is that in some cases, particle sizes (in ranges larger than 25 micrometres) were recorded which were considerably larger than the size for which the corresponding filter was rated. The number of particles in such cases are considered only a trace amount compared to the total number of particles below 25 micrometres in size and the readings are possibly attributable to errors in recording equipment and/or the agglomeration of small particles into apparent larger particles. Figure 18 shows that use of the 10 or 25 micrometre filter did not substantially reduce the number of particles in the 2-10 micrometre range but did for the 10-25 micrometre range. This fact taken together with the previous data (Figure 17) showing that the R.T. Ferrograph could not detect failures using 10 and 25 micron filters indicates that the R.T. Ferrograph is: (a) not capable of detecting particles in the 2-10 micron range and, (b) is most sensitive at detecting particles in the 10-25 micrometre range. On the other hand Figure 17 shows that the GEOM and the SOA do show a gradual increase in reading during the 10 and 25 micrometre filtration series indicating a better responsiveness than the R.T. Ferrograph to particles in the 2-10 micrometre range.

Bearing Fatigue Tests

10. As described in the Method of Test Section, a series of five tests were run with double flanged outer race, single flanged inner race, sixty millimetre bore roller bearings (SKF NJ212). These bearings had eight of the sixteen roller elements removed and the inner raceway etched to accelerate the failure. After the initial failure (fatigue spall) the damage was allowed to propagate halfway around the inner raceway to insure a high level of particle contamination.

11. The data generated during these bearing fatigue tests are presented in Figure 19. The arrows indicate when initial spall failure took place. In the "no filter" case, the bearing failed due to excessive cage wear rather than fatigue spalling. The R.T. Ferrograph results show no indication of failure at the 40 micrometre level or below. At the 75 micrometre and the no filter levels the increasing trend in reading level indicates a failure in progress. On the other hand both the GEOM and the SOA show increasing wear trends with time at all filtration levels except for the ten micrometre level. It can also be seen in Figure 19 that the recirculation test results indicate a reduction in reading with decreasing filter rating for all the monitors. However, the effect is most dramatic with the R.T. Ferrograph.

12. The UTRC X-ray wear metal monitor was run only in the case in which no filter was used and therefore the results are not shown in Figure 19. Comparison of it with the other monitors is shown in Figure 20. All of the oil monitors show the same trends, indicating a high initial increase and then leveling off. However, the PPM level of iron indicated by the X-ray unit was much lower than that of the emission spectrometer.

13. Again as in the scoring tests the preponderance of wear particles are in the 2-10 and 10-25 micrometre range as shown in Figure 21. Unlike the scoring tests, the ten micrometre filter was able to trap particles in the 2-10 micrometre range. This was perhaps due to the fact that the bearing tests ran much longer which allowed the filter sufficient time to "plug up" with larger particles and effectively become a finer filter. Also unlike the scoring tests, there appears to be no relationship between the response of the R.T. Ferrograph and the particle size distribution. For example in the case of the 75 and 40 micrometre filter tests where the particle count distributions are very similar, the R.T. Ferrograph responds (see Figure 19) positively to the 75 micrometre test and negatively to the 40 micrometre test. On the other hand the GEOM and SOA show a positive response in all cases where the particle count is high in the 2-10 and 10-25 micrometre ranges and a negative response when the particle count is low in these ranges. In addition the bearing test results on the GEOM and SOA detectors are consistent with those in the scoring tests.

14. Appendix D tabulates the data generated during the Bearing Fatigue Tests.

Summary of the Effectiveness of the Oil Monitors at Various Filtration Levels

15. The data presented thus far was reviewed for each monitor and a subjective judgement was made to determine the effectiveness of each monitor at the various levels of filtration. These results are given in Table I for both the disc scoring and bearing fatigue tests. If a monitor was not evaluated at a particular filtration level, an N.T. (Not Tested) is indicated in the table. "Marginal" indicates that the data showed a possible, but not clearly definable, trend towards indicating a failure. The tests run at the coarser level of filtration show all of the oil monitors clearly indicating a failure. As the level of filtration becomes finer, the ability of all of the oil monitors lessens as shown in Table I. Also Table I shows that the GEOM and the SOA are effective over the widest filtration range. The R.T. Ferrograph is ineffective below the 40 micrometre filtration level.

Comparison of Various Severity of Wear Indices

16. Three Severity Indices described earlier were compared for a representative disc scoring test, namely the test in which the 75 micrometre

filter was used. The values of A_L, A_S, SI_1, SI_2, and SI_3 are given in Appendix C and SI_1, SI_2, SI_3 are plotted graphically in Figure 22. It can be seen that the SI_1 ratio is a poor indicator of failure because at extremely low values of A_L and A_S where very little particle generation is taking place, large values in severity index occur, which falsely indicates a failure. This confirms the results obtained in Figure 14 where SI_1 is plotted for various slide-to-roll ratio tests. Figure 22 shows that the other two indices performed well in indicating the first scoring failure. SI_2 and SI_3 both show an initial increase, a leveling off and then a slight decrease.

Effects of Oil Volume on the Outputs (A_L AND A_S) of the R.T. Ferrograph

17. The data generated during all of the tests shows that at filtration levels of less than 40 micrometres the R.T. Ferrograph outputs and Severity Indices are not sufficiently large or sensitive to indicate a failure or abnormal wear. This problem may possibly be resolved by passing a larger volume of oil through the R.T. Ferrograph and consequently depositing an increased number of both large and small particles. Data has been generated to show the relationship between the oil volume passed through the R.T. Ferrograph and the outputs of the R.T. Ferrograph. Figure 23 shows that increasing the oil volume significantly increases the magnitudes of the outputs A_L and A_S. It can also be seen that this relationship is linear (a linear regression analysis yields a correlation coefficient of 0.99 for all cases). The effects of oil filtration on the output magnitude can therefore be compensated for by increasing the oil sample volume. The data in Figure 23 was generated using the oil remaining after the completion of the 25 micrometre filtration test for both disc scoring and bearing fatigue tests.

Effects of Oil Volume on the Sensitivity of the R.T. Ferrograph Severity Index

18. Figure 23 shows that the relationship between the percentage area covered for both the large and small particles and oil volume passed through the R.T. Ferrograph is linear. These relationships can therefore be expressed as follows:

$$A_L = m_L V_o + b_L \qquad \text{Equation (1)}$$

$$A_S = m_S V_o + b_S \qquad \text{Equation (2)}$$

where m_L = is slope of the line for large particles
m_S = is slope of the line for small particles
A_L = Percent area covered - Large particles
A_S = Percent area covered - Small particles
b_L = constant (A_L intercept)
b_S = constant (A_S intercept)
V_o = Volume of oil passed through R.T. Ferrograph.

19. The Severity Index (SI_3) is defined as:

$$SI_3 = A_L^2 - A_S^2$$

then substituting equations (1) and (2) yields

$$SI_3 = (m_L\ Vo)^2 - (m_S\ Vo)^2 \quad \text{Equation (3).}$$

The assumption was made that $b_L = b_S = 0$ since the R.T. Ferrograph autozero cycle does this automatically at the start of each cycle. The sensitivity of this Severity Index with respect to oil volume can be characterized by taking the derivative of Equation (3) with respect to Vo. This yields

$$\frac{d\ (SI_3)}{d\ Vo} = 2\ Vo\ (m_L^2 - m_S^2) \quad \text{Equation (4)}$$

The sensitivity of this Severity Index is therefore dependent upon the difference of the squares of the rates of increase of the R.T. Ferrograph outputs, A_L and A_S, and on the quantity of oil passed through the system. The effect of the parameter $(m_L^2 - m_S^2)$ with respect to SI_3 per unit volume of oil is shown graphically in Figure 24. The lines in Figure 24 for $(m_L^2 - m_S^2) = 0.110$ and $(m_L^2 - m_S^2) = 0.097$ are for the rolling element bearing fatigue and disc scoring test data presented in Figure 23. Figure 24 illustrates that the sensitivity of the Severity Index (SI_3) can be adjusted with variations in oil volume to accomodate the operating characteristics of the equipment being monitored. For example it can be seen that if $(m_L^2 - m_S^2) = 0$ then the Severity Index (SI_3) is insensitive since the rates of change in percent area covered per unit volume of oil between large and small particles are equal. As the parameter $(m_L^2 - m_S^2)$ increases, then the rate of change of SI_3 per unit volume of oil increases more rapidly with increasing volume of oil flow. It should be noted that for a normal wear regime, the parameter $(m_L^2 - m_S^2)$ will remain essentially constant and as a system progresses towards failure it will increase. Therefore, for any particular system, the oil volume selected should be in a sensitivity range which will indicate changes in the Severity Index (SI_3) without severely affecting the repeatability of the reading. For example, helicopter transmissions are expected to generate many more large particles than small particles in a manner such that $(m_L^2 - m_S^2)$ is a large number. In this case it is desirable to use a small volume of oil to compensate for the high sensitivity of the Severity Index (SI_3). Conversely if the equipment generates particles such that $(m_L^2 - m_S^2)$ is small, then a large volume of oil is desirable in order to obtain sufficient sensitivity to provide an adequate measure of the wear in the system being monitored. In addition, if the filtration level used in a particular system is so fine that $(m_L^2 - m_S^2)$ is very close to or equal to zero then an increase in oil volume, no matter how large, will not influence the Severity Index (SI_3).

Correlation of the R.T. Ferrograph with the Analytical Ferrograph

20. The Analytical Ferrograph, as previously described, is a laboratory device which is used to precipitate wear particles, from an oil sample, onto a glass slide (Ferrogram) for microscopic examination. The area at

which the particles are first deposited onto the Ferrogram is an important parameter for wear indication and is analogous to the A_L output of the R.T. Ferrograph. For comparative purposes, Ferrograms were produced from oil samples obtained during the disc scoring and rolling element bearing fatigue tests conducted at the 75 micrometre filtration levels. In addition, Ferrograms were produced for each of the recirculating series after the tests. Comparisons were then made for the A_L (R.T. Ferrograph output) and the height of the entry deposit on a Ferrogram for readings and samples obtained simultaneously. Figure 25 shows a comparison of the results obtained in the disc test and Figure 26 shows a comparison of the results obtained in the bearing tests. These figures show a good correlation of trends between the R.T. Ferrograph A_L output and the entry deposit height. This lends confidence to the ability of the R.T. Ferrograph to accurately reflect characteristics of the Analytical Ferrograph.

LIST OF SYMBOLS AND ABBREVIATIONS USED IN TEXT

Symbol/Abbreviations

A_L	-	R.T..Ferrograph output - percent area covered at large particle position of the precipitator tube
A_S	-	R.T. Ferrograph output - percent area covered at small particle position of the precipitator tube
GEOM	-	General Electric Oil Monitor
GRTM	-	Geared Roller Test Machine
SI_1	-	Severity of Wear Index = $\frac{A_L}{A_S}$
SI_2	-	*Severity of Wear Index* = $A_L (A_L - A_S)$
SI_3	-	Severity of Wear Index = $A_L^2 - A_S^2$
SOA	-	Spectrometric Oil Analysis by Emission Spectrometer
UTRC X-ray	-	United Technologies Research Center X-ray Wear Metal Monitor

FIGURE 1 GEARED ROLLER TEST MACHINE

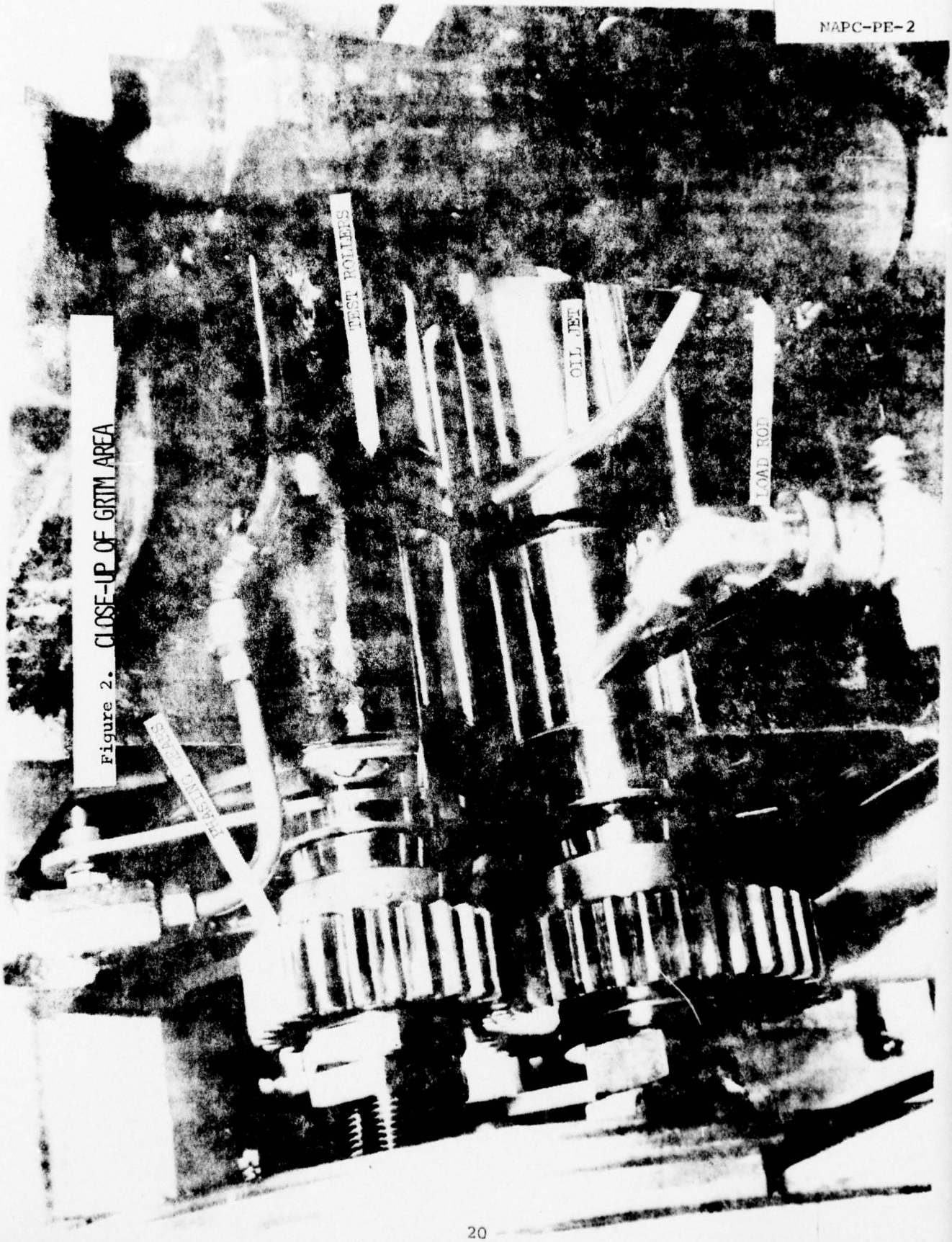

Figure 2. CLOSE-UP OF GRTM AREA

Figure 3. **GEARED ROLLER TEST MACHINE SCHEMATIC**

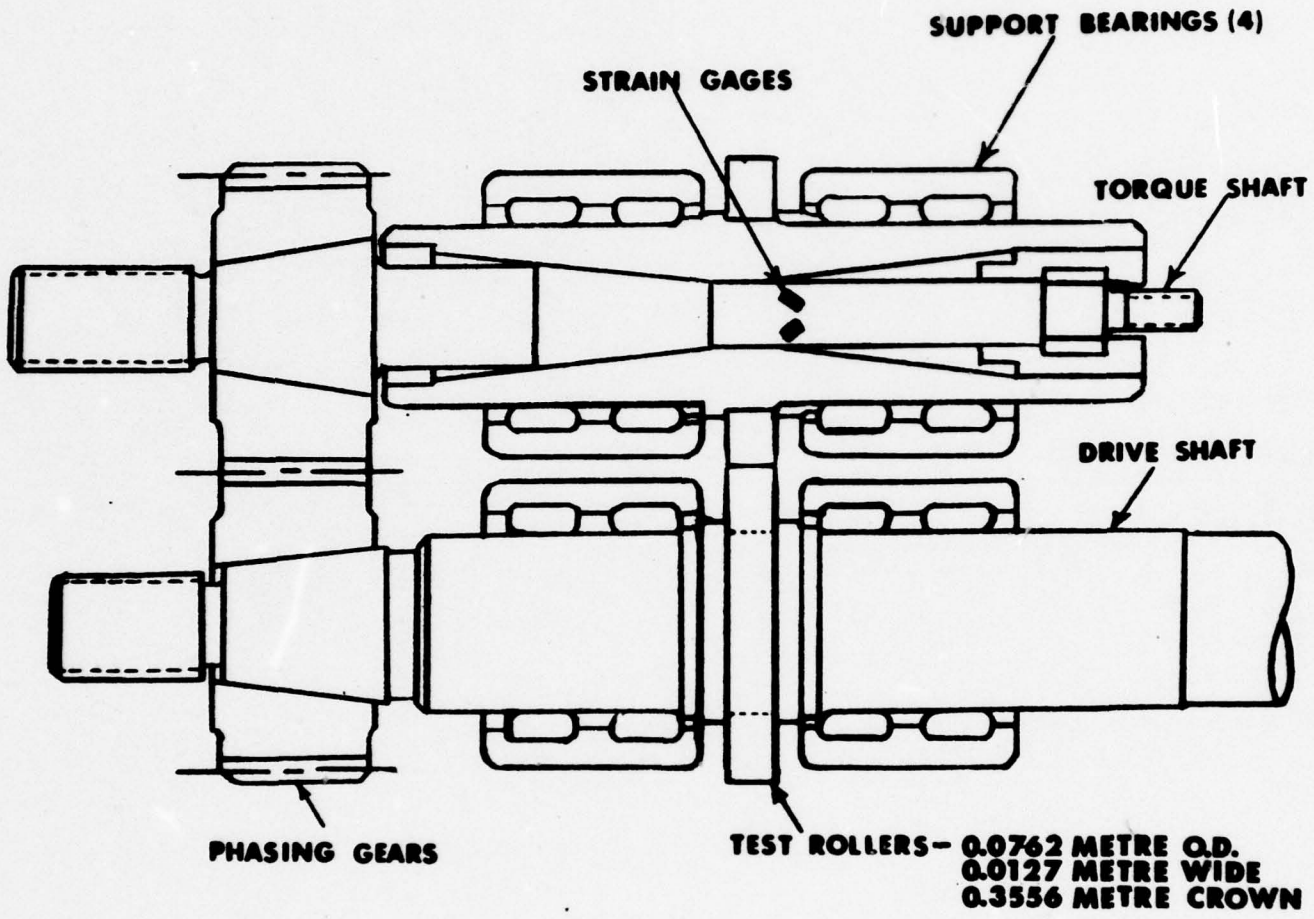

NAPC-PE-2

Figure 4. DEFINITION OF VELOCITY TERMS FOR GRTM

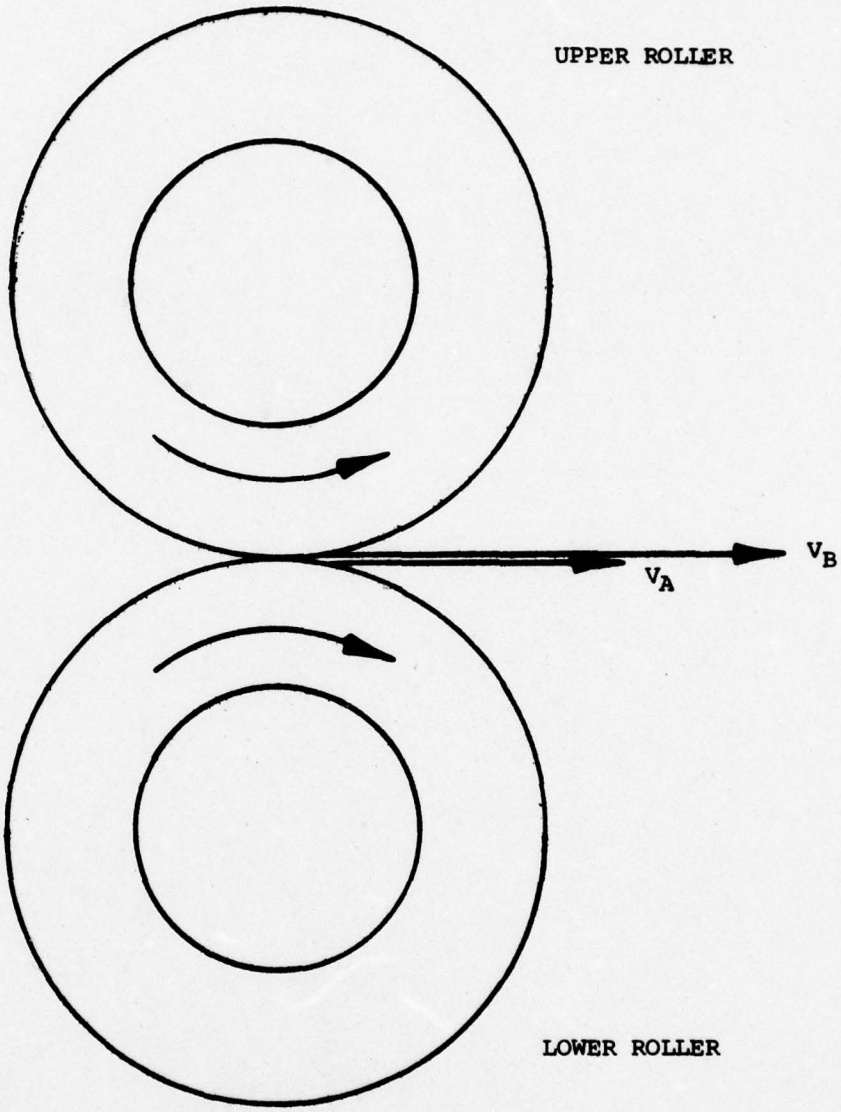

V_B = Tangential Velocity of Upper Rollers

V_A = Tangential Velocity of Lower Roller

$V_A + V_B = R$ = Rolling Velocity

$|V_A - V_B| = S$ = Sliding Velocity

$\frac{S}{R}$ = Slide-To-Roll Ratio

Figure 5. APPLIED TEST ROLLER LOAD VS. MAXIMUM HERTZ STRESS FOR GRTM

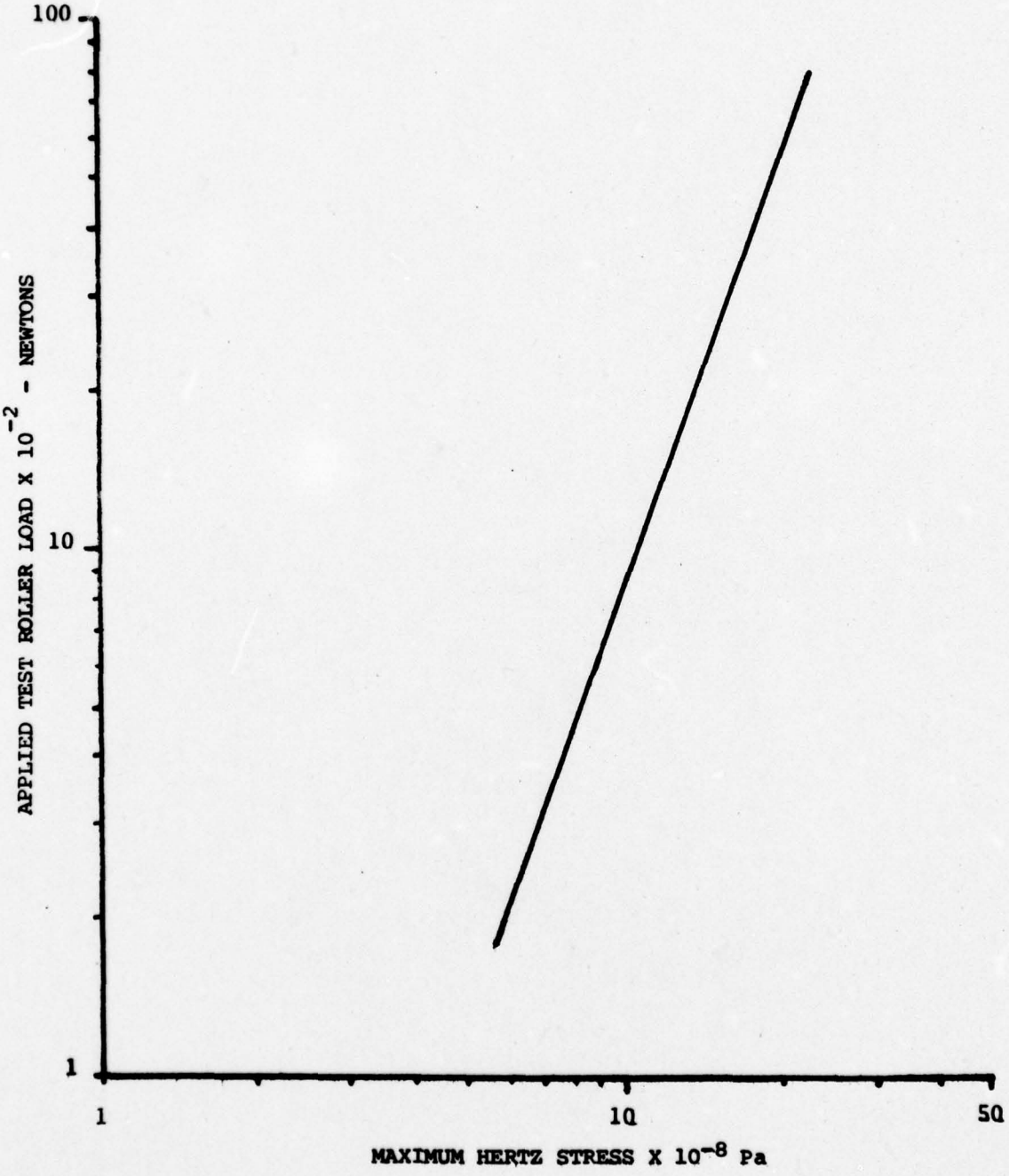

Figure 6. **BEARING HOUSING ADAPTOR FOR GRTM**

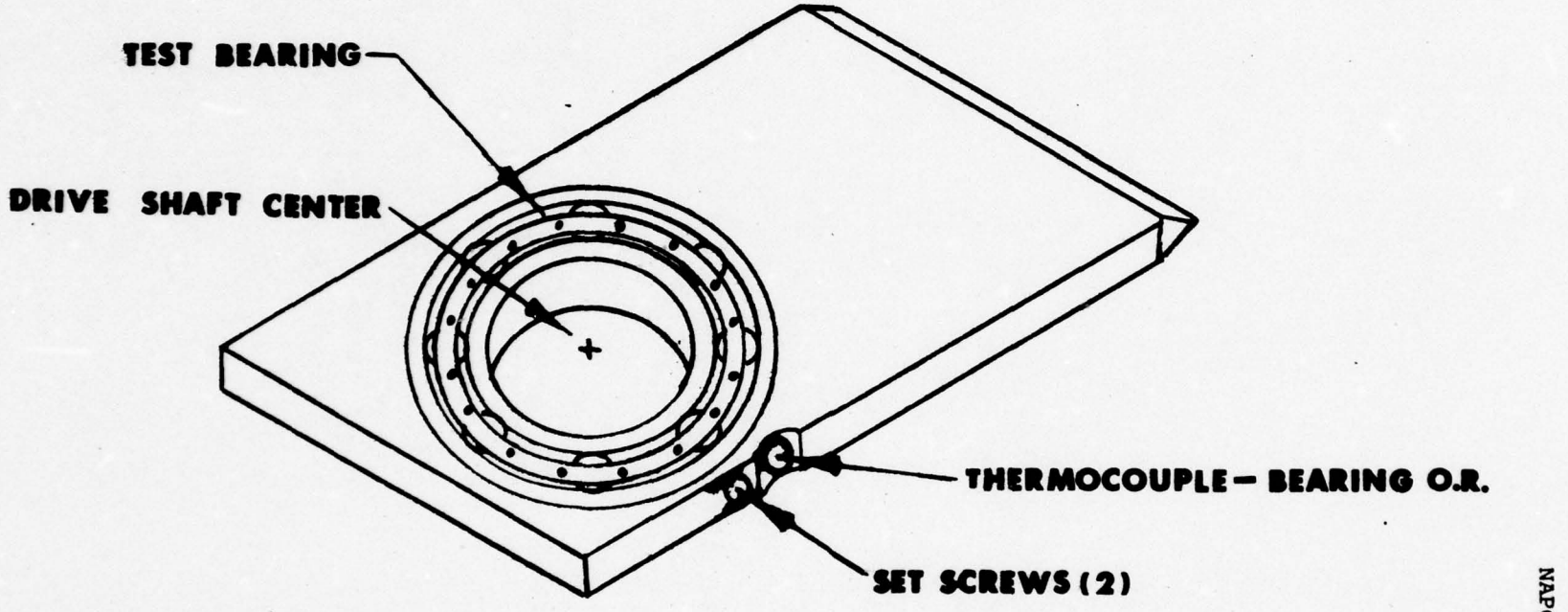

NAPC-PE-2

FIGURE 7.

GEARED ROLLER TEST MACHINE LUBRICATION SYSTEM SCHEMATIC FOR OIL MONITOR EVALUATION

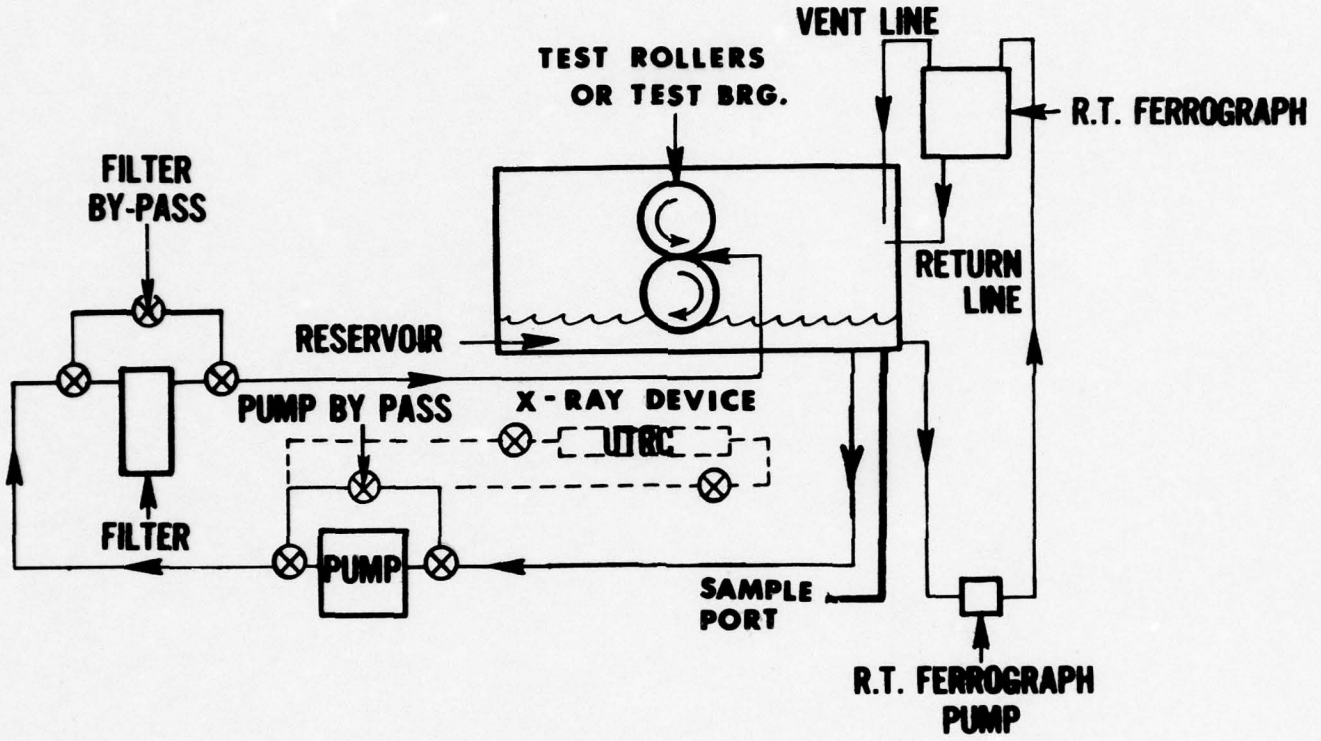

BENCH DEVICES

1. LIGHT SCATTERING (GEOM)
2. EMISSION SPECTROSCOPY
3. ANALYTICAL FERROGRAPH

FIGURE 8. INSTALLATION OF R.T. FERROGRAPH ON THE GRTM BENCH TESTER

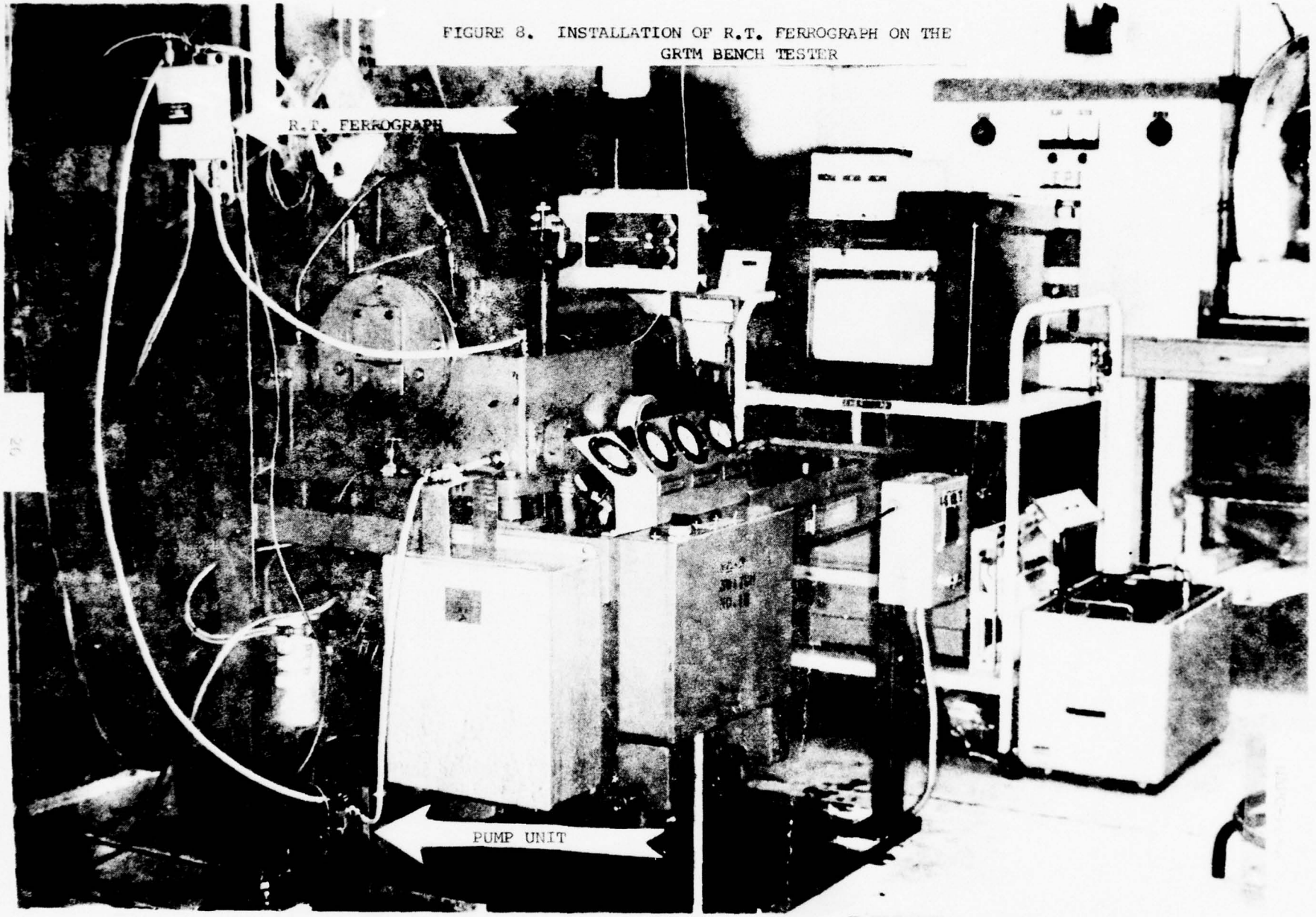

Figure 9. INTERNAL OIL FLOW & OPTICAL SYSTEM OF RT FERROGRAPH

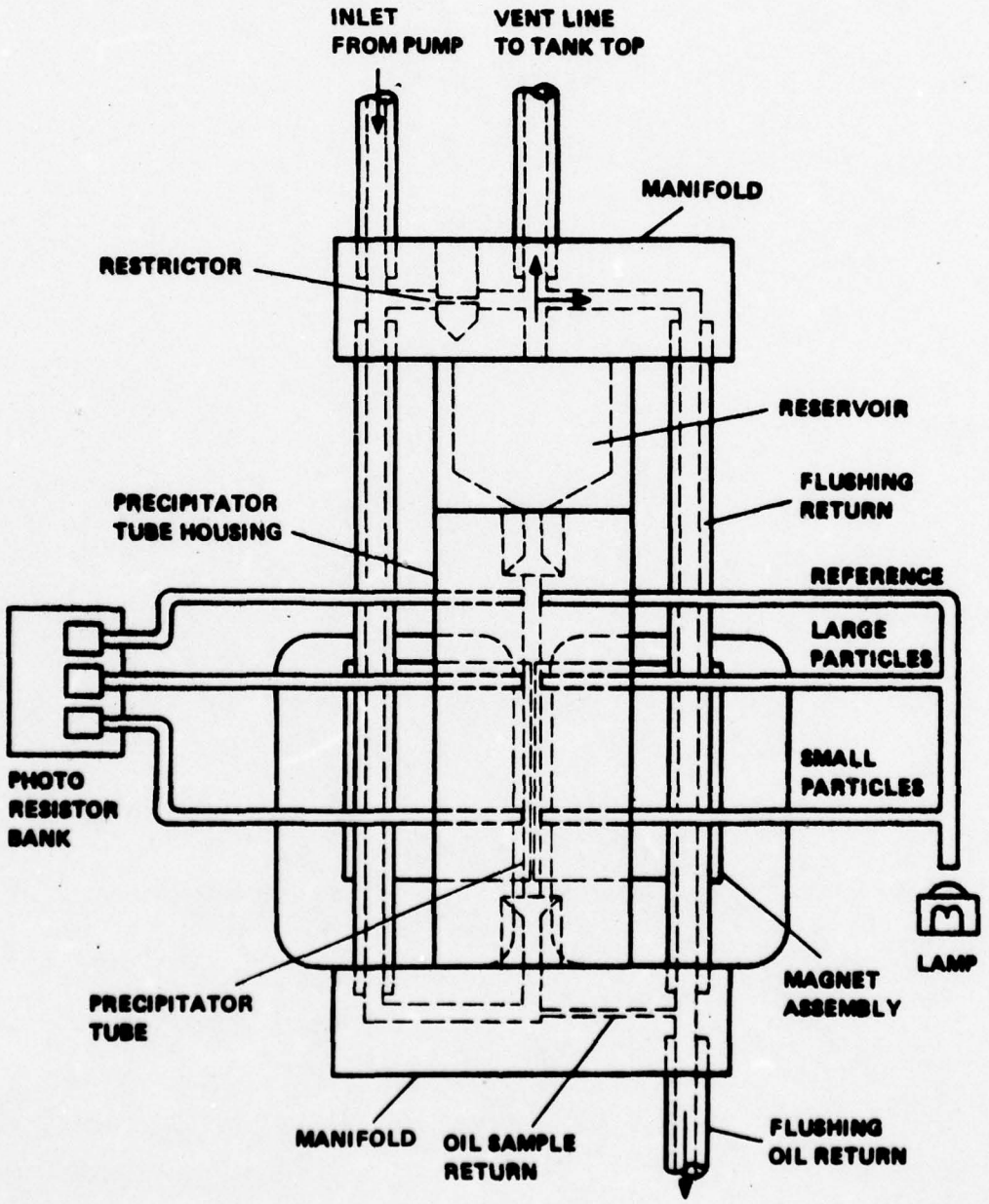

Figure 10.

GENERAL ELECTRIC OIL MONITOR SENSOR HEAD

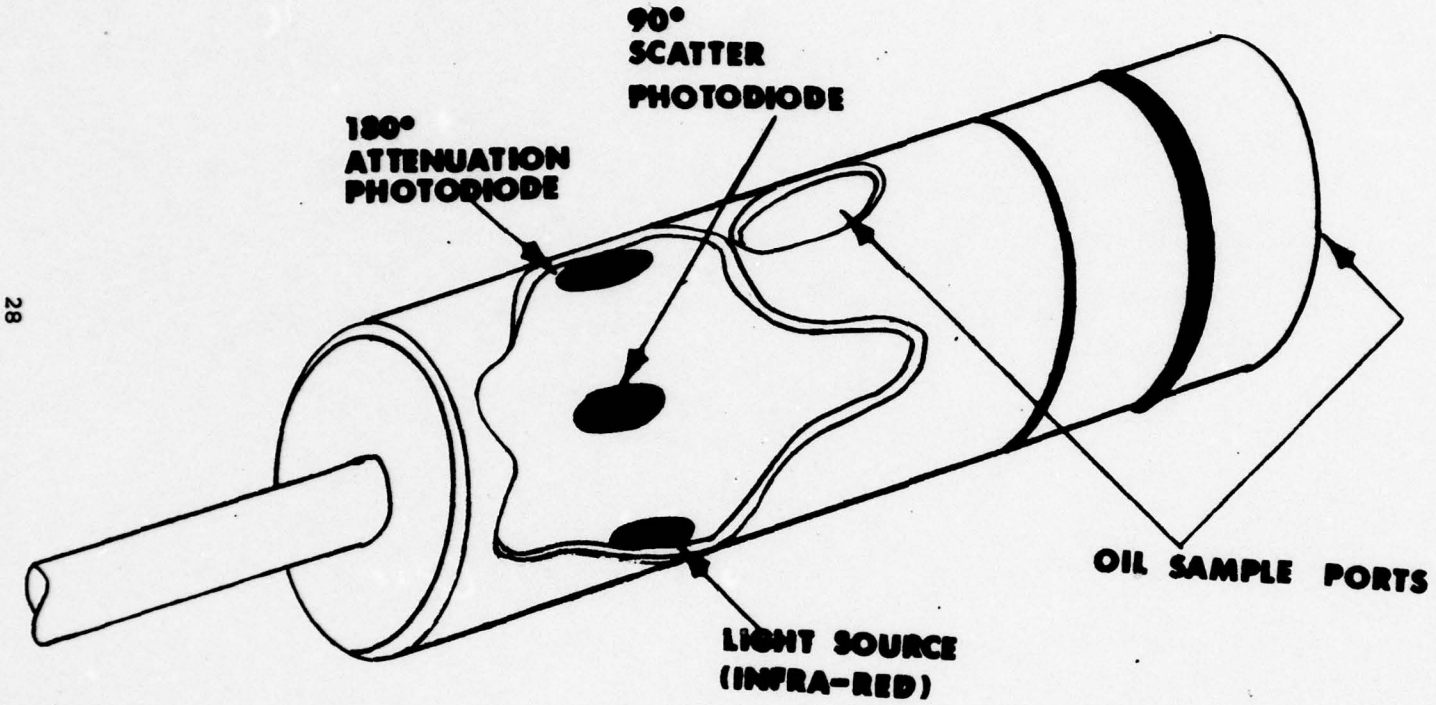

NAPC-PE-2

FIGURE 11. SCHEMATIC OF UNITED TECHNOLOGIES RESEARCH CENTER X-RAY WEAR METAL MONITOR

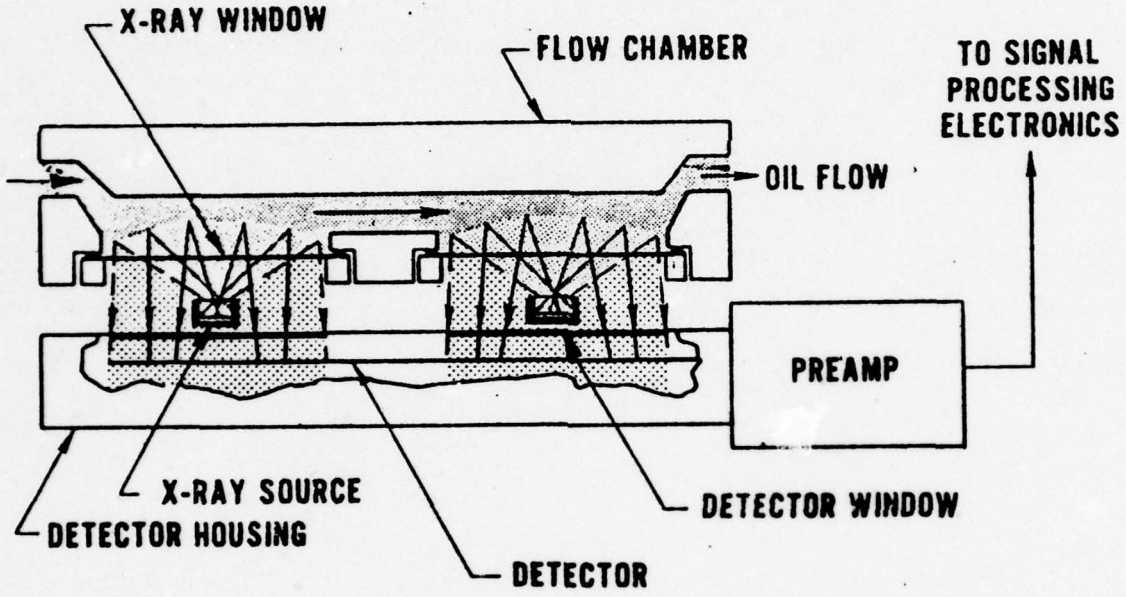

Figure 12. **COMPARISON OF INITIAL AND FINAL FATIGUE SPALLS**

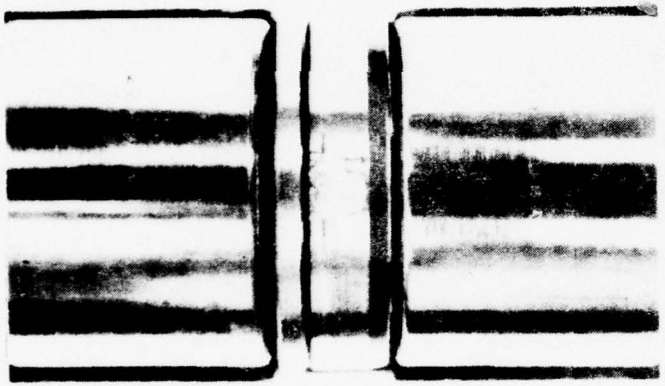

TYPICAL INITIAL FATIGUE SPALL

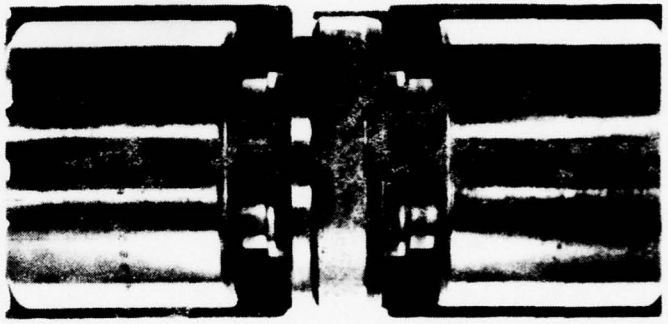

TYPICAL FINAL FATIGUE SPALL

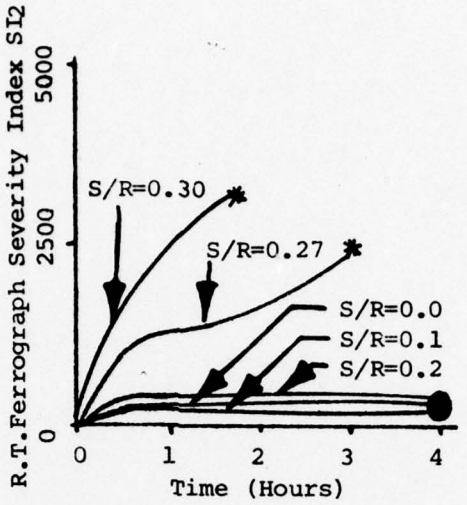

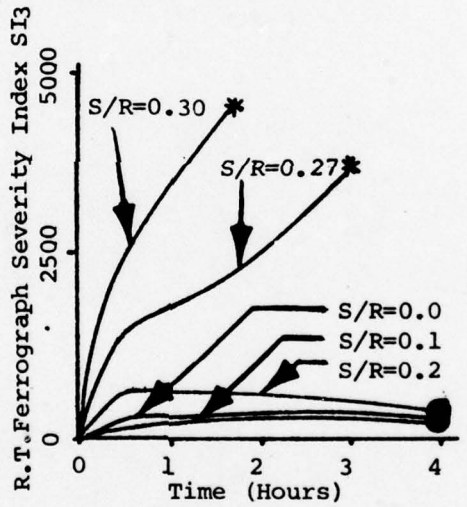

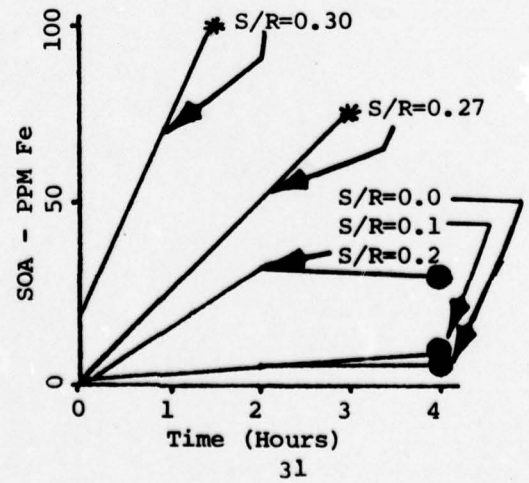

LEGEND

● No Failure

✱ Scoring Failure

FIGURE 13: COMPARISONS OF THE R.T. FERROGRAPH READINGS AND SOA FOR VARIOUS SLIDE-TO-ROLL RATIOS ON THE GRTM

FIGURE 14: COMPARISON OF THE R.T. FERROGRAPH SEVERITY INDEX (SI_1) FOR VARIOUS SLIDE-TO-ROLL RATIOS ON THE GRTM

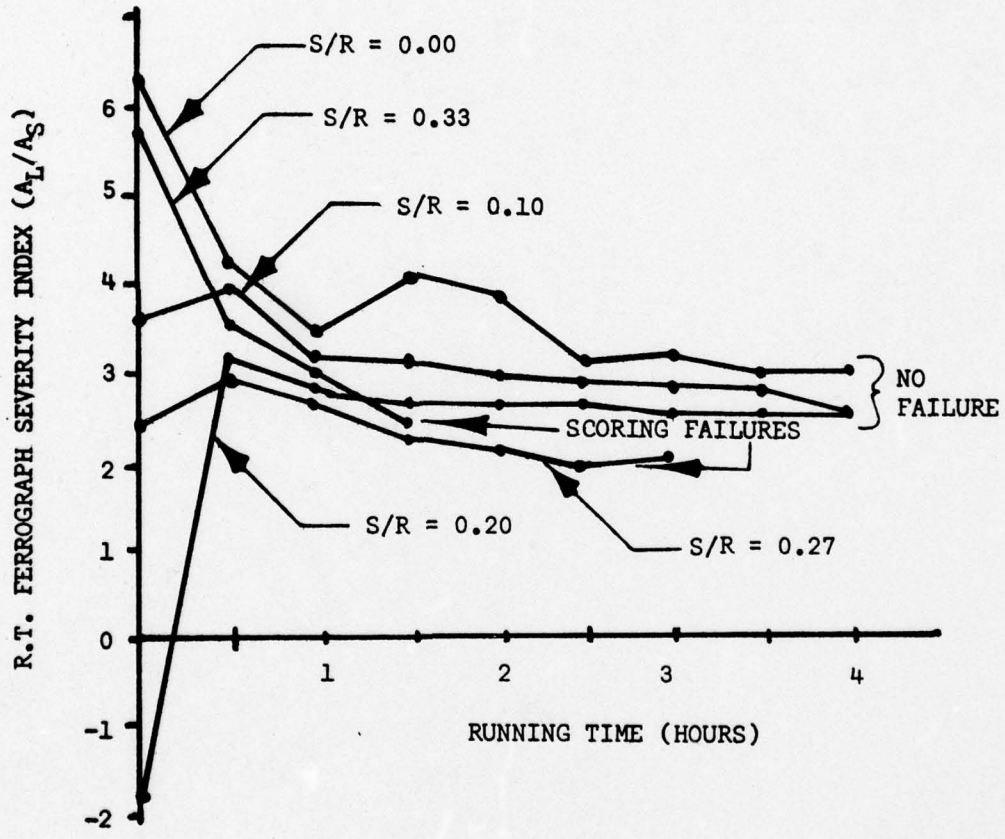

Figure 15. **OIL MONITOR READING VS PERCENT RUNNING TIME FOR DISC SCORING TEST WITH NO FILTRATION**

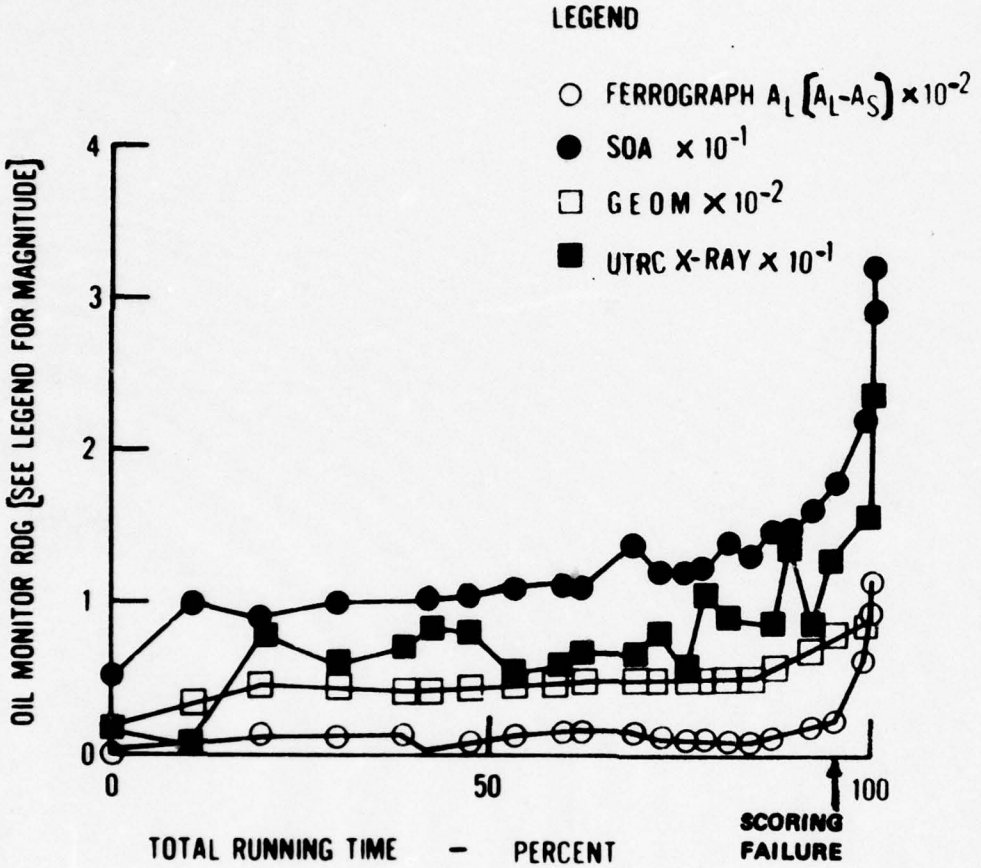

FIGURE 16. NOMINAL MICROMETRE RATING FOR VARIOUS ENGINE OIL FILTERS

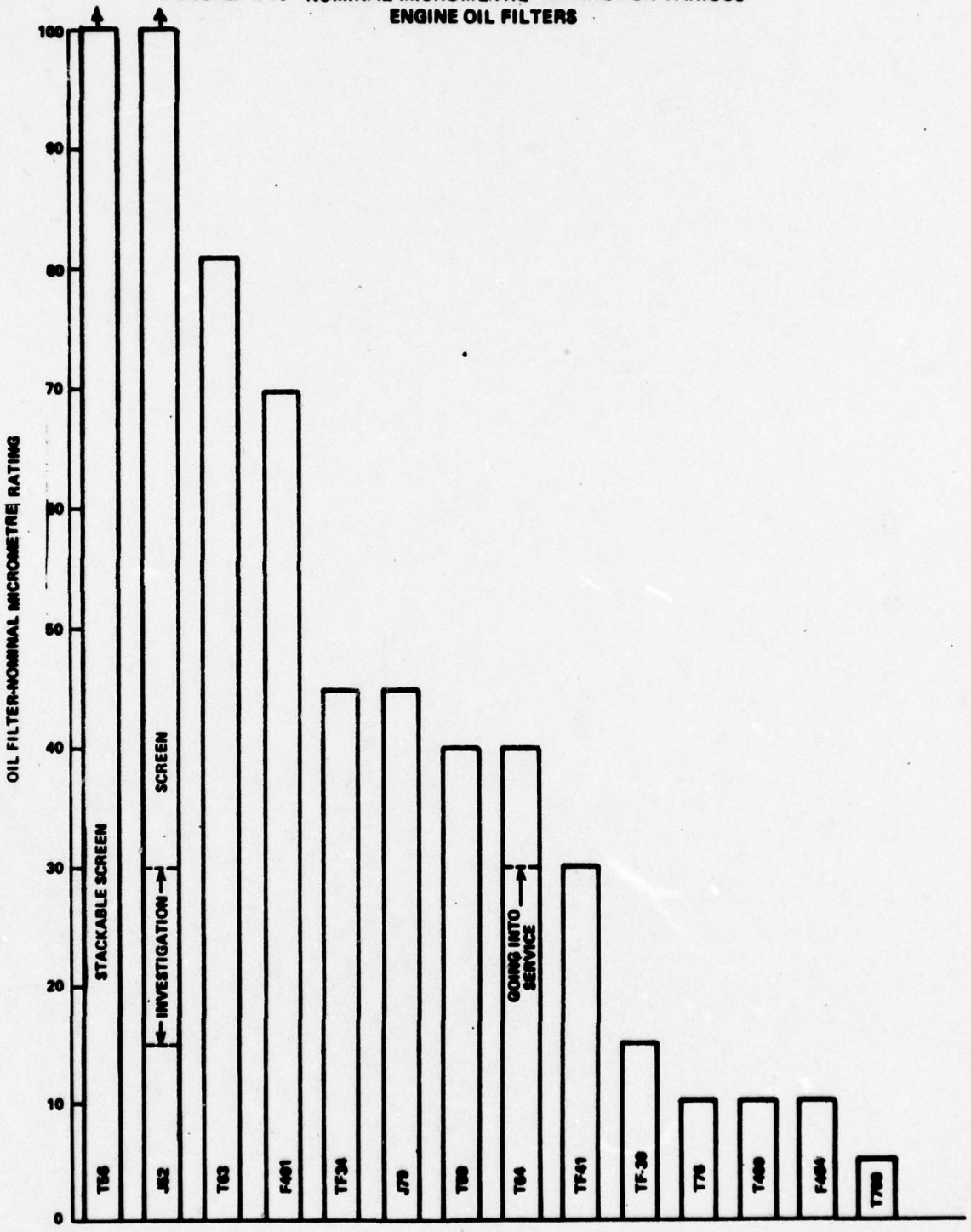

FIGURE 17. OIL MONITOR READINGS VS PERCENT RUNNING TIME FOR THE DISC SCORING TEST SERIES

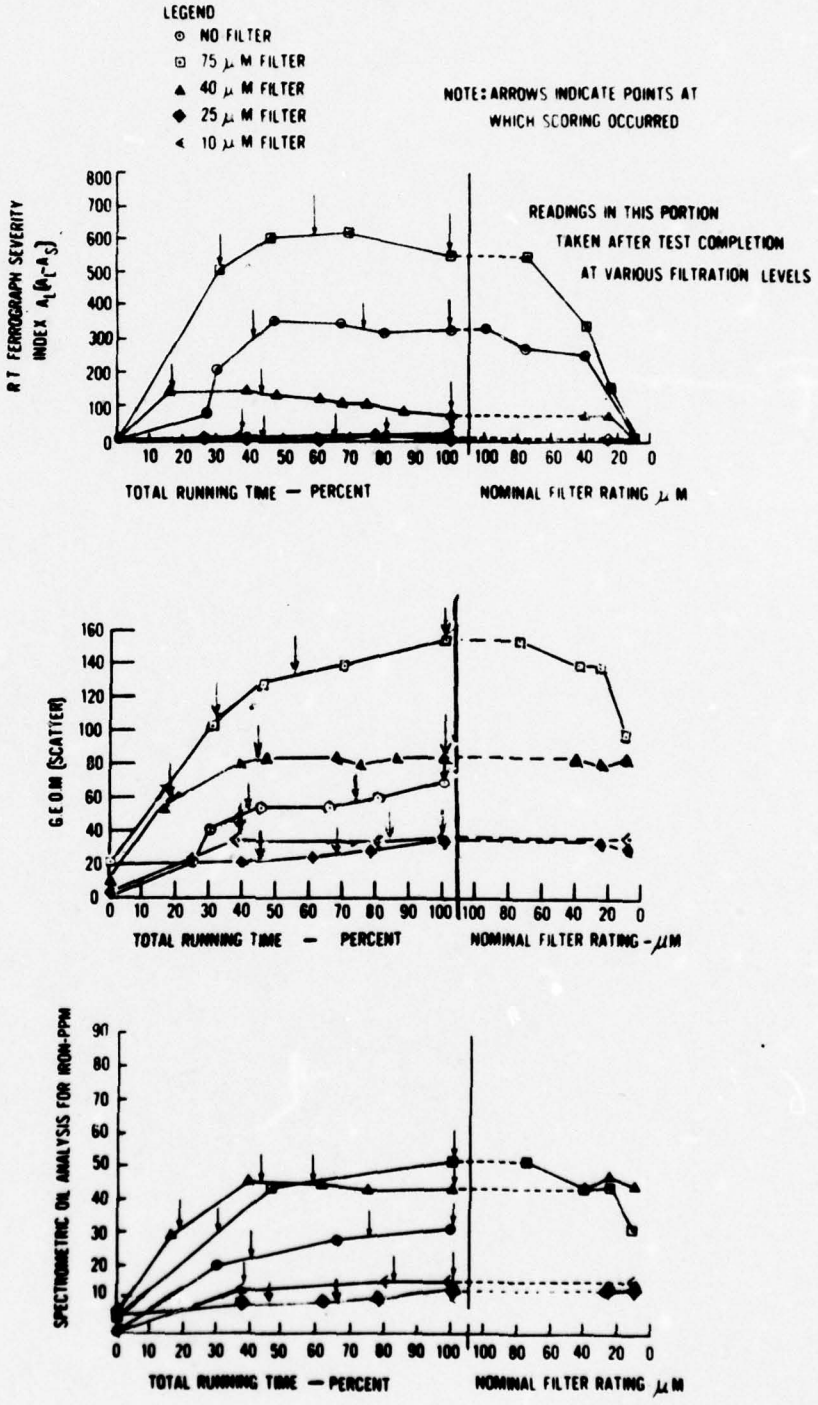

FIGURE 18. WEAR PARTICLE DISTRIBUTION AT VARIOUS FILTRATION LEVELS FOR THE DISC SCORING TEST SERIES

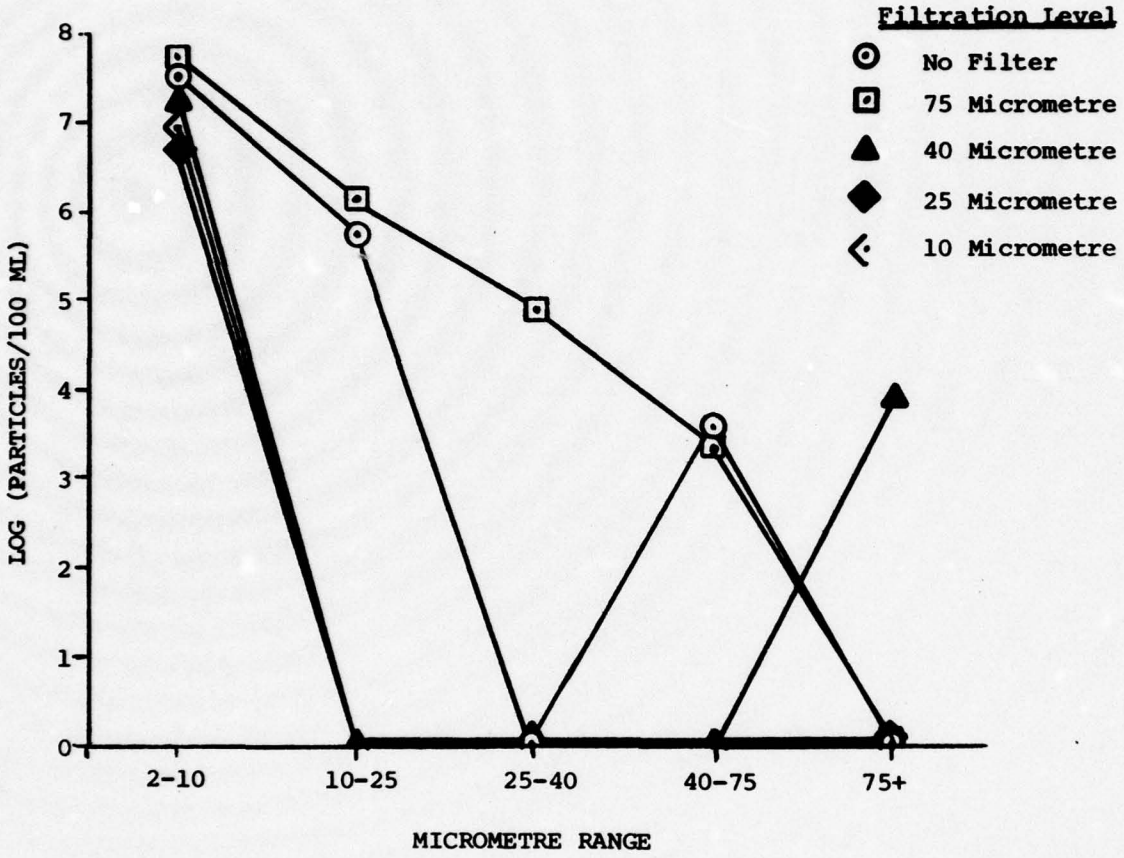

FIGURE 19. OIL MONITOR READINGS VS PERCENT RUNNING TIME FOR THE BEARING TEST SERIES

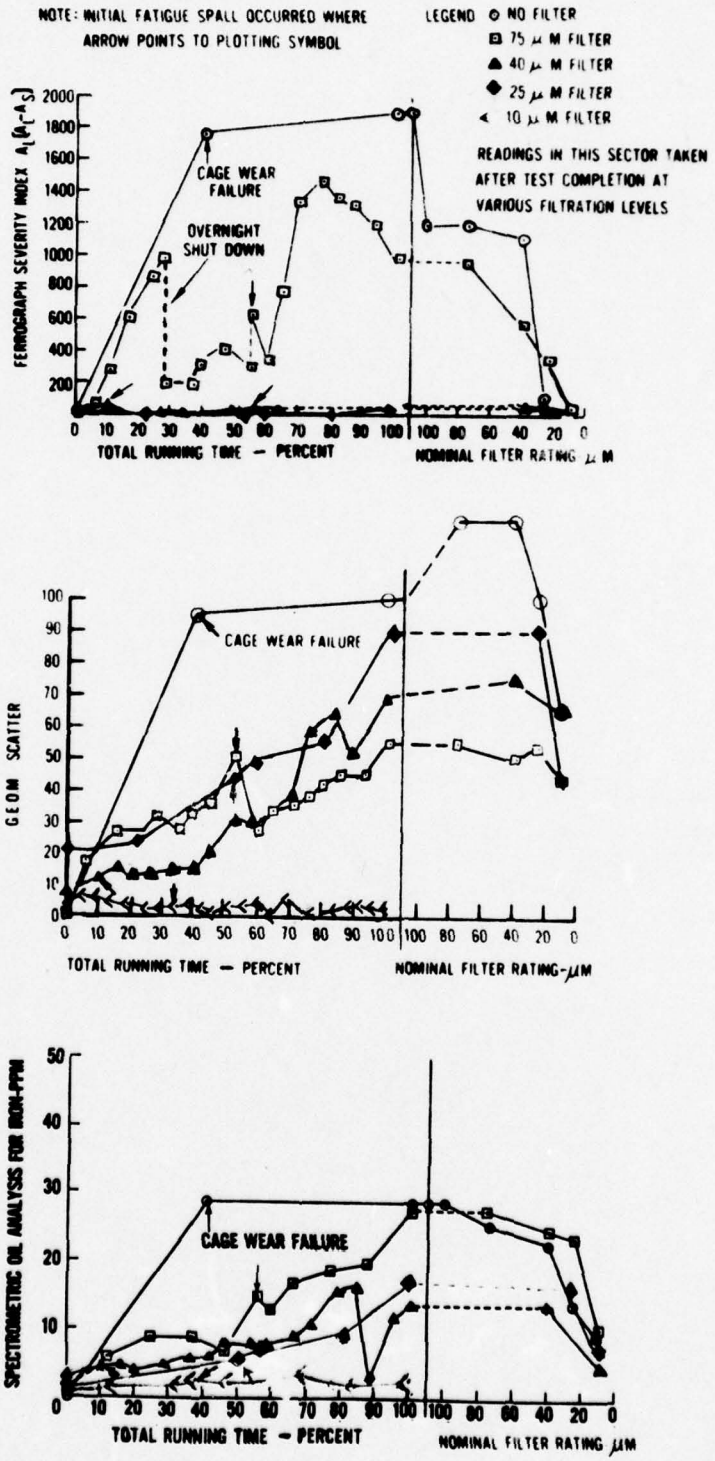

Figure 20. OIL MONITOR READING VS PERCENT RUNNING TIME FOR BEARING TEST WITH NO FILTRATION

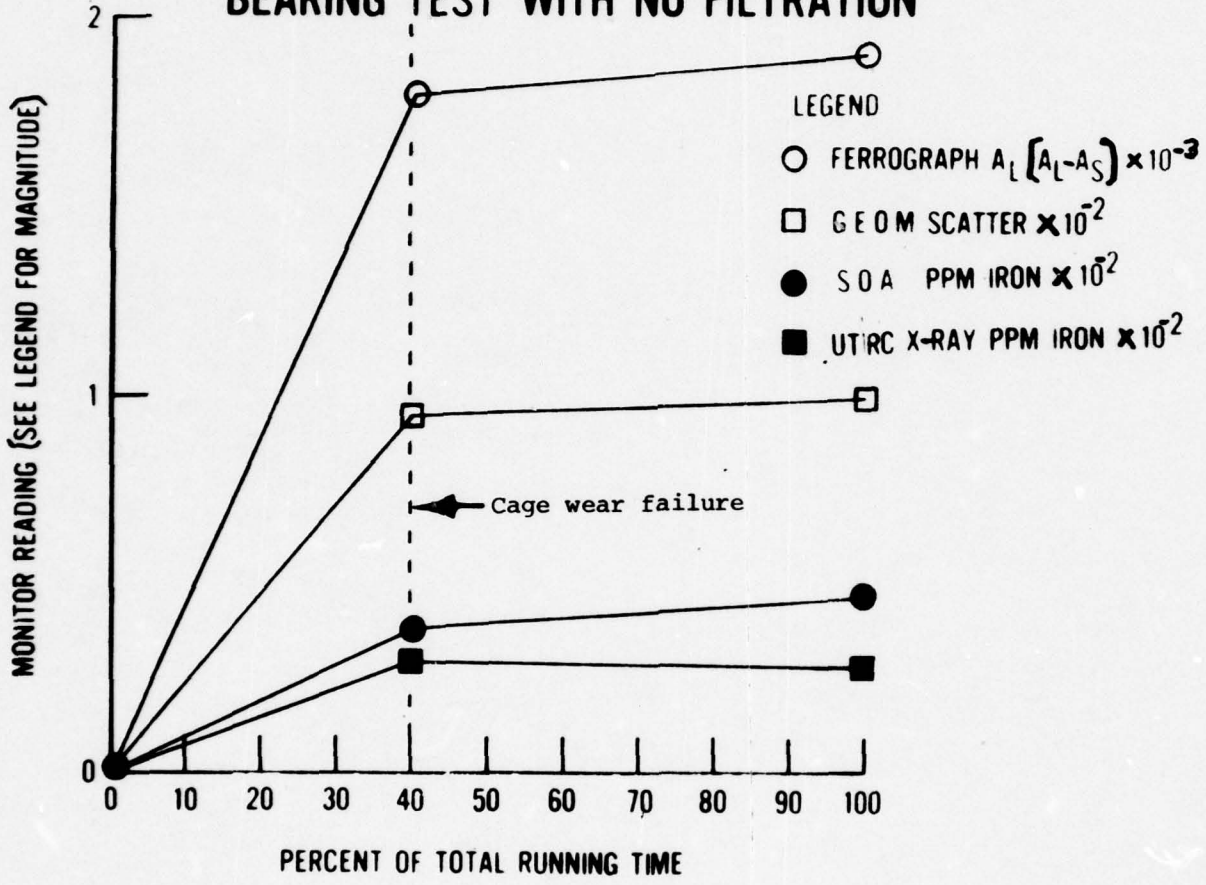

FIGURE 21. WEAR PARTICLE DISTRIBUTION AT VARIOUS FILTRATION LEVELS FOR THE BEARING FATIGUE TEST SERIES

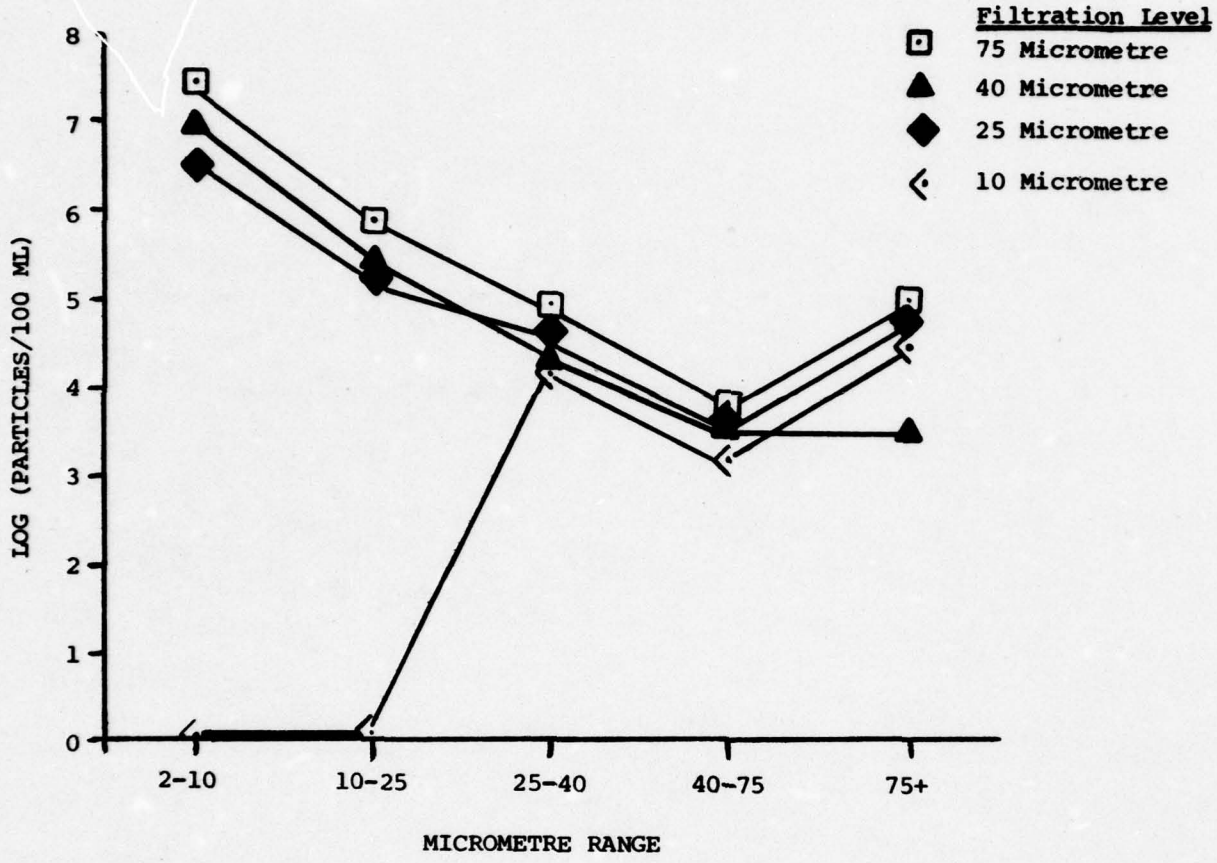

Figure 22. COMPARISON OF VARIOUS SEVERITY INDICES FOR DISC SCORING

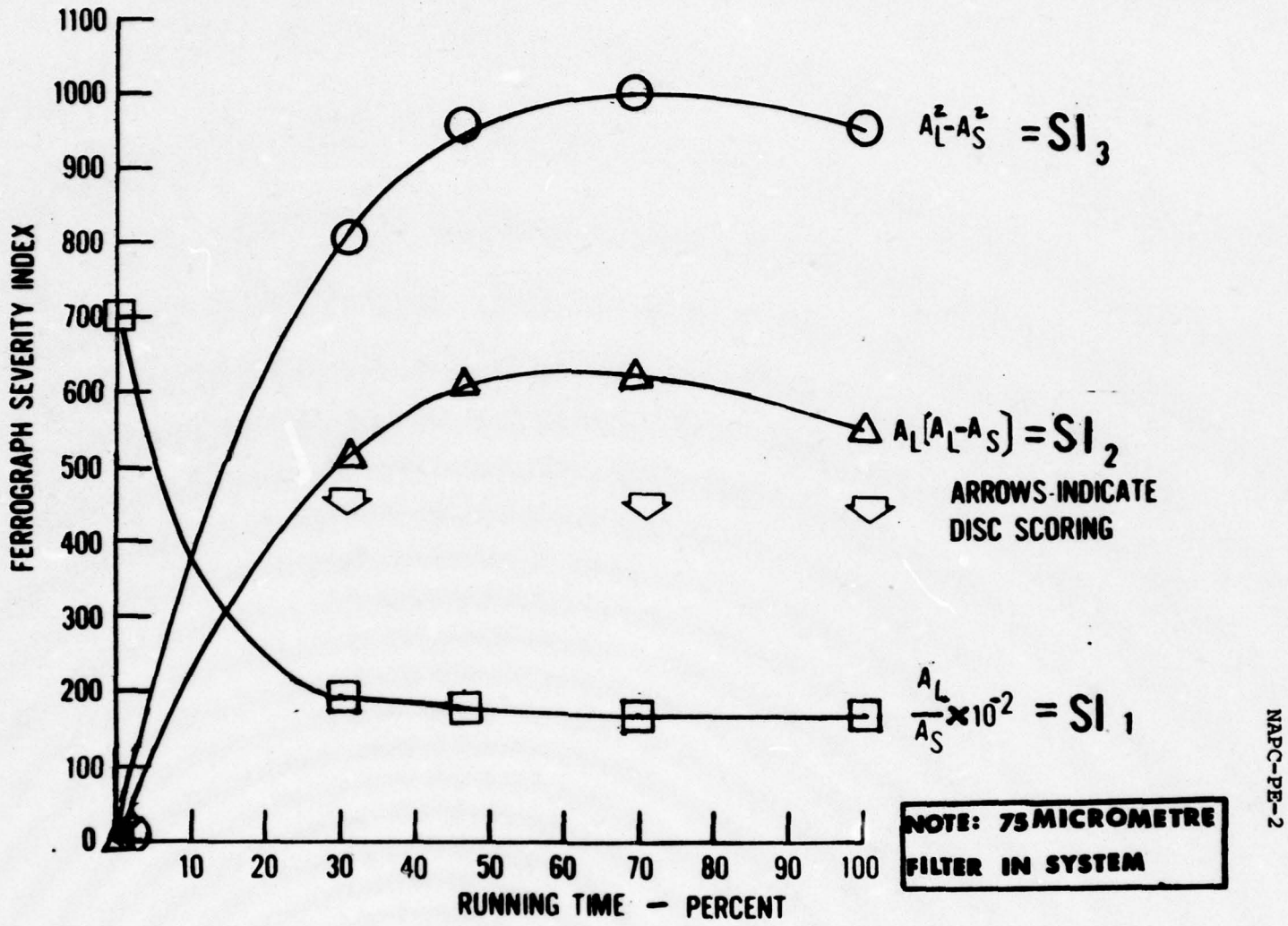

NAPC-PE-2

FIGURE 23. EFFECT OF R.T. FERROGRAPH READING VS. OIL VOLUME FLOW THROUGH SYSTEM

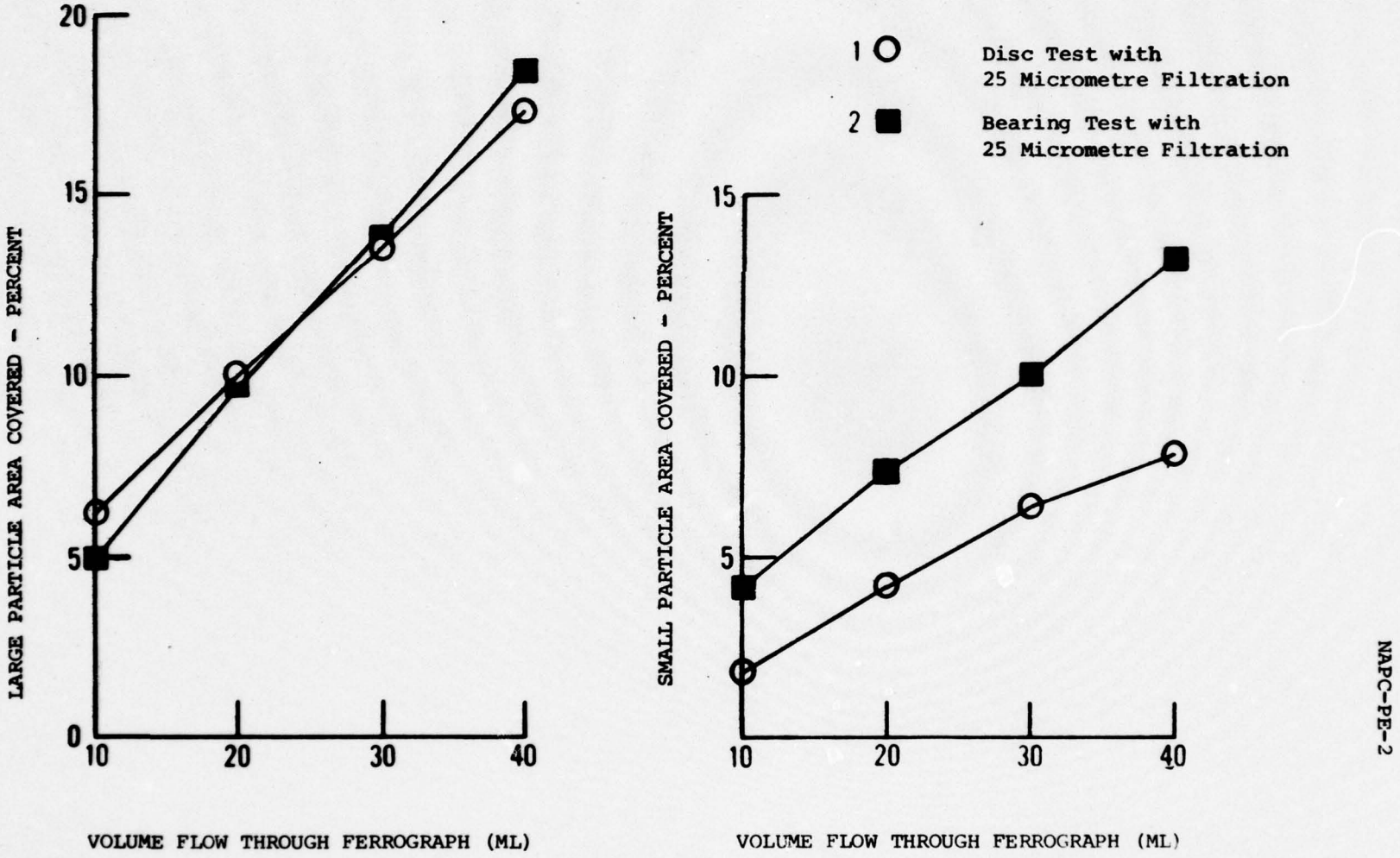

FIGURE 24. SENSITIVITY OF THE SEVERITY INDEX WITH CHANGES IN OIL VOLUME AS AFFECTED BY DIFFERENCES IN PRECIPITATION RATE BETWEEN LARGE AND SMALL PARTICLES

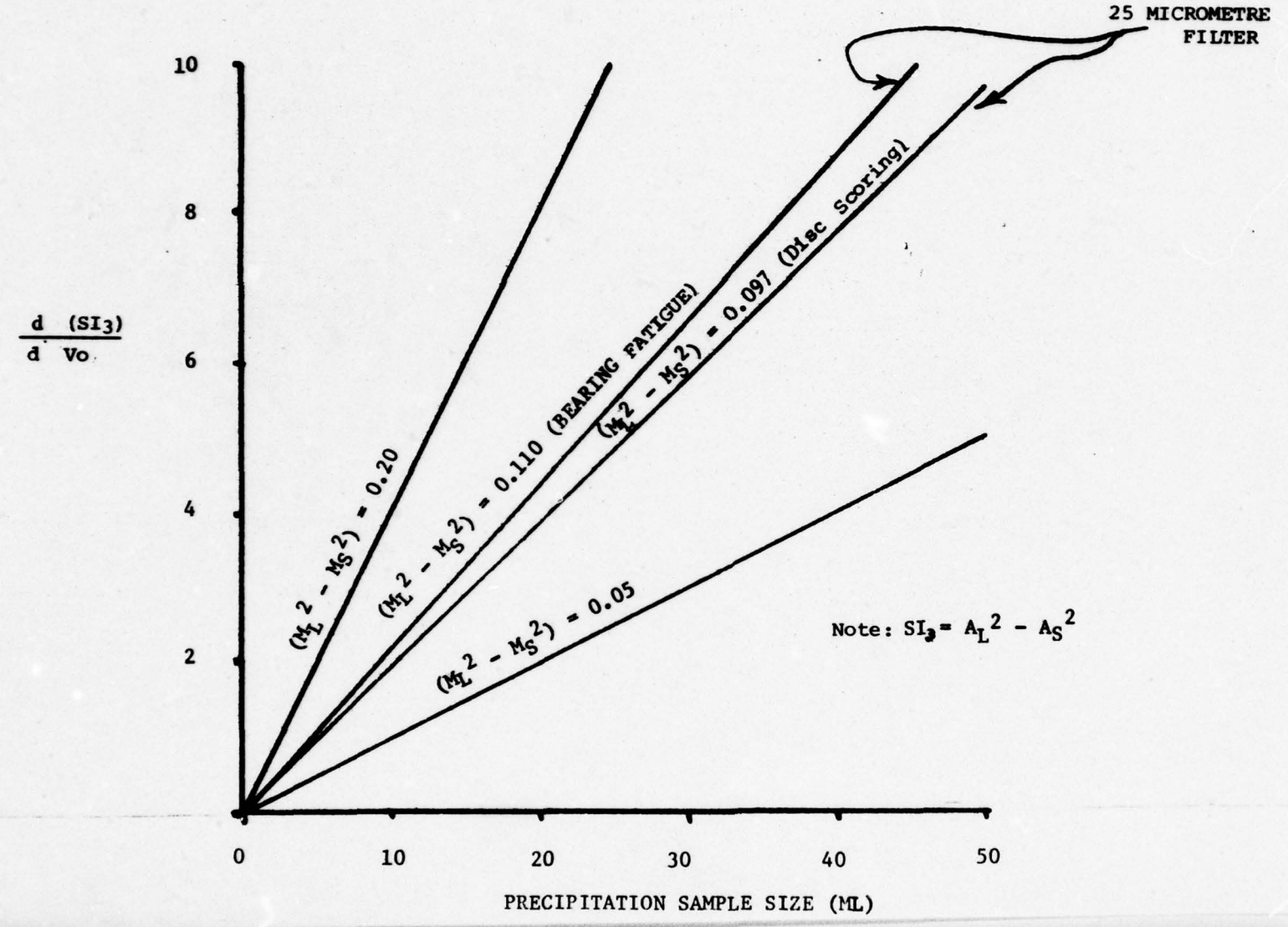

NAPC-PE-2

FIGURE 25. COMPARISON OF R.T. FERROGRAPH AND ENTRY DEPOSIT HEIGHT FOR A DISC SCORING TEST RUN AT THE 75 MICROMETRE FILTRATION LEVEL

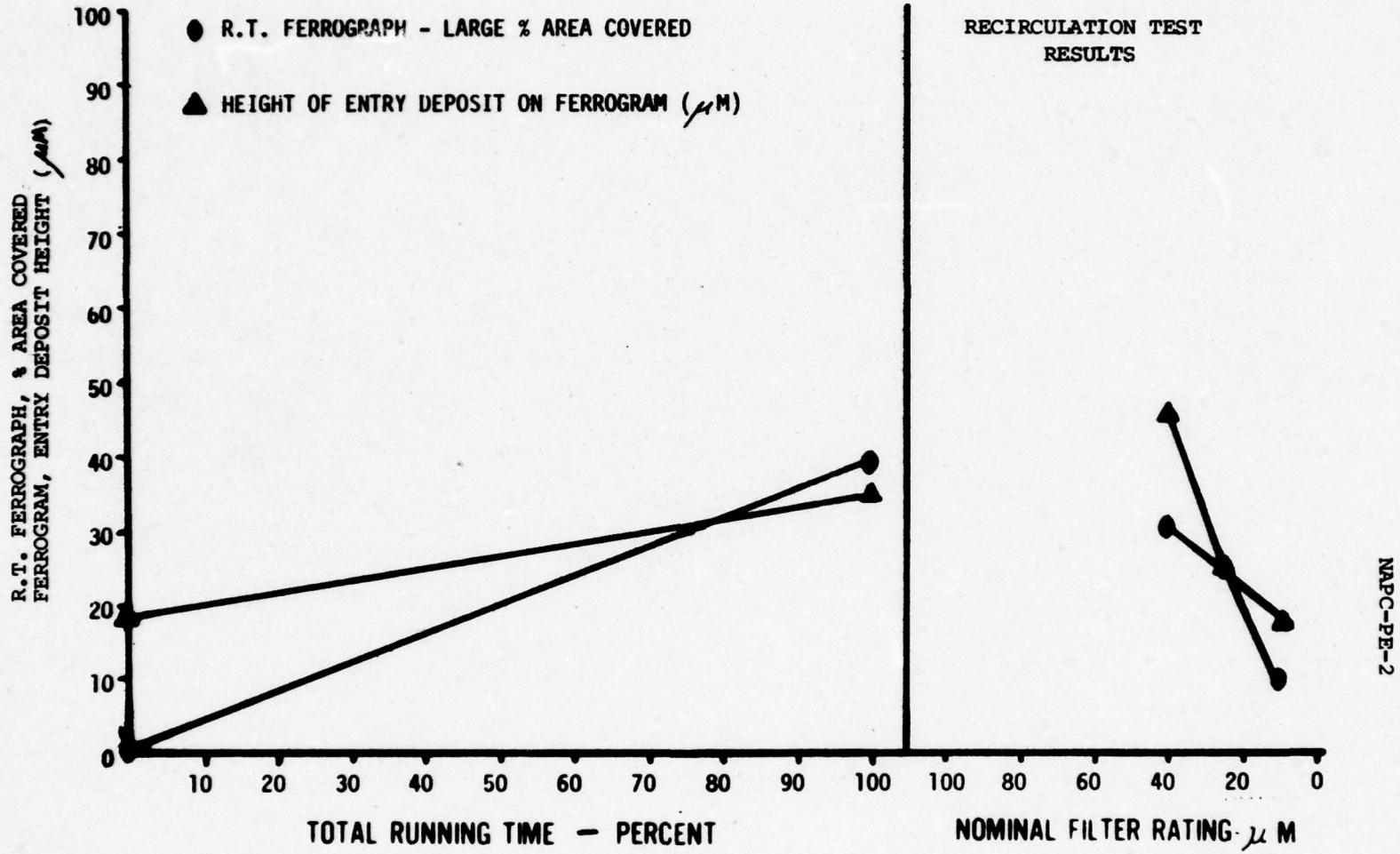

NAPC-PE-2

Figure 26. COMPARISON OF R.T. FERROGRAPH AND ENTRY DEPOSIT HEIGHT FOR BEARING RUN TO ULTIMATE FAILURE AT THE 75 MICROMETRE FILTRATION LEVEL

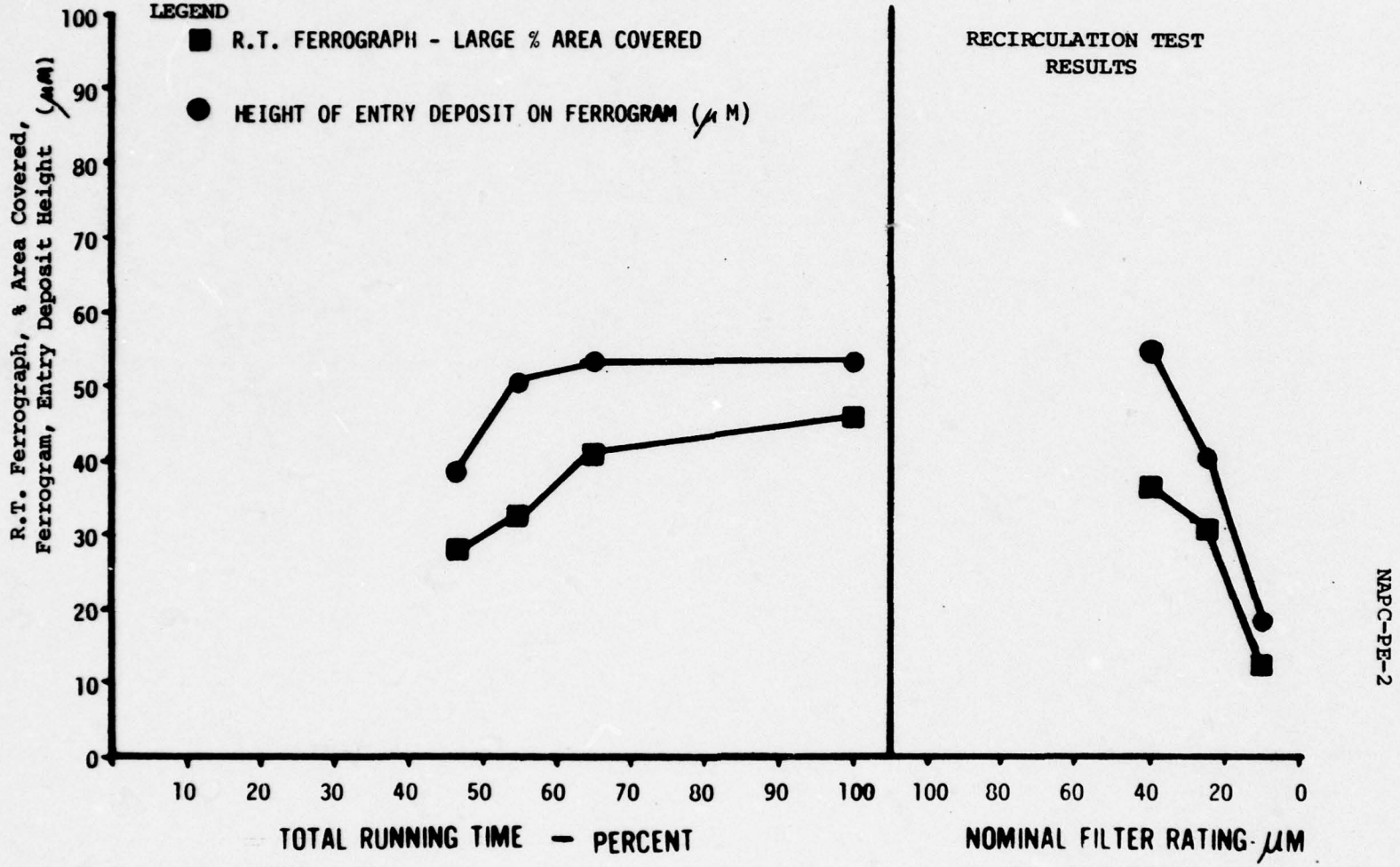

NAPC-PE-2

TABLE I

EFFECTIVENESS OF THE OIL MONITORS AT VARIOUS FILTRATION LEVELS

A. Bearing Fatigue

Monitor	Filtration Level (Micrometre)				
	None	75	40	25	10
R. T. Ferrograph	Sat.	Sat.	Unsat.	Unsat.	Unsat.
SOA	Sat.	Sat.	Sat.	Unsat.	Unsat.
GEOM	Sat.	Sat.	Sat.	Sat.	Unsat.
UTRC X-ray	Sat.	N.T.	Unsat.	N.T.	N.T.

B. Disc Scoring

Monitor	Filtration Level (Mircrometre)				
	None	75	40	25	10
R. T. Ferrograph	Sat.	Sat.	M	Unsat.	Unsat.
SOA	Sat.	Sat.	Sat.	M	M
GEOM	Sat.	Sat.	Sat.	M	M
UTRC X-ray	Sat.	N.T.	N.T.	N.T.	N.T.

LEGEND: **Sat.** - Satisfactory

Unsat. - Unsatisfactory

N.T. - Not Tested

M - Marginal

REFERENCES

1. REPORT: Tauber, T., A Report on the State-Of-The-Art in Chip Detector Technology; Technical Development Co., Glenholden, Pa. 19036, July 1976.

2. REPORT: Beerbower, A., Mechanical Failure Prognosis Through Oil Debris Monitoring, U.S. Army Air Research and Development Laboratory, Ft. Eustis, Va. 23604; January 1975.

3. REPORT: Wescott, V.C. and Wright, R.W., Final Report: Real Time Ferrograph For Application on Jet Engines In A Test Cell Environment; Naval Air Propulsion Test Center, Trenton, NJ 08628; July 1974.

4. REPORT: Bowen, E.R. and Wescott, V.C., Wear Particle Atlas, Naval Air Engineering Center, Lakehurst, N.J. 08733; July 1976.

5. REPORT: Miner, J.R. and Packer, L.L., X-ray Wear Metal Monitor, Air Force Aero Propulsion Laboratory, Wright-Patterson AFB, Ohio, 45433; January 1975.

APPENDIX A

DISC SCORING TEST SERIES

Load 4741 N (1066 lbs)
No Filtration
V_A (Tangential Velocity of Lower Roller) = 3.49 m/sec (137.4 ips)

Elapsed Time (Hrs.)	Slide/Roll Ratio	R.T. FERROGRAPH A_L	A_S	SI_1	SI_2	SI_3	SOA PPM (Fe)
0.0	0.33	1.7	0.3	5.7	2.4	2.8	18
0.5	0.33	52.0	15.0	3.5	1924.0	2479.0	
1.0	0.33	63.0	22.0	2.9	2583.0	3485.0	
1.5*	0.33	74.5	32.8	2.3	3107.0	4474.0	100
0.0	0.27	3.2	1.3	2.46	6.1	8.6	2
0.5	0.27	40.0	13.5	2.96	1060.0	1418.0	
1.0	0.27	45.3	17.0	2.66	1282.0	1763.0	24
1.5	0.27	51.1	23.6	2.17	1405.0	2054.0	
2.0	0.27	58.5	28.8	2.03	1738.0	2593.0	49
2.5	0.27	62.1	32.8	1.89	1820.0	2781.0	
3.0*	0.27	70.9	35.8	1.98	2489.0	3745.0	75
0.0	0.20	0.7	-0.4	-1.75	0.8	0.3	1
0.5	0.20	24.5	8.2	2.99	399.4	533.0	
1.0	0.20	26.7	9.5	2.80	459.2	622.4	
1.5	0.20	26.9	10.2	2.60	449.2	619.6	
2.0	0.20	25.0	9.7	2.60	382.5	530.9	33
2.5	0.20	23.0	8.9	2.60	324.3	449.8	
3.0	0.20	21.4	8.7	2.50	271.8	382.3	
3.5	0.20	21.0	8.4	2.50	264.6	370.4	
4.0**	0.20	19.0	7.8	2.40	212.8	300.2	29
0.0	0.10	0.7	0.2	3.50	0.4	0.5	1
0.5	0.10	10.1	2.7	3.70	74.7	94.7	
1.0	0.10	11.9	3.7	3.20	97.6	127.9	
1.5	0.10	13.7	4.4	3.10	127.4	168.3	
2.0	0.10	13.5	4.8	2.80	117.5	159.2	3
2.5	0.10	13.0	4.8	2.70	106.6	146.0	
3.0	0.10	14.2	5.3	2.70	126.4	173.6	
3.5	0.10	14.3	5.2	2.75	130.1	177.5	
4.0**	0.10	14.2	5.6	2.50	122.1	170.3	4
0.0	0.0	3.2	0.5	6.40	8.6	10.0	0
0.5	0.0	12.7	3.0	4.23	123.2	152.3	
1.0	0.0	13.0	3.8	3.42	119.6	154.6	
1.5	0.0	16.0	4.0	4.00	192.0	240.0	
2.0	0.0	18.0	4.8	3.75	237.6	301.0	3
2.5	0.0	18.7	5.9	3.17	239.4	314.9	
3.0	0.0	17.5	5.5	3.18	210.0	276.0	
3.5	0.0	15.9	5.5	2.89	165.4	222.6	
4.0**	0.0	14.8	5.1	2.90	143.6	193.0	6

* Scored at end of test
**No scoring

APPENDIX B

ELLIPTICAL GEAR TEST

Load to 26980 N (6066 lbs)
No Filtration
Slide/Roll Ratio - sinusoidally varied between 0 and 0.2

W_A (rotational velocity of driving gear) - 91.6 rps (875 rpm)

Elapsed Time (Hrs.)	R.T. FERROGRAPH					GEOM		SOA	UTRC X-RAY
	A_L	A_S	SI_1	SI_2	SI_3	Scatter	Attentuation	PPM(Fe)	PPM(Fe)
0.0	0.5	-0.1	-5.00	0.06	0.24	18	10	5	1.6
1.2	-	-	-	-	-	36	17	10	0.93
2.1	5.8	2.9	2.00	16.8	25.2	45	20	9	7.6
3.2	5.3	3.3	1.61	10.6	17.2	43	22	10	6.0
4.1	5.0	2.5	2.00	12.5	18.8	42	21	10	7.0
4.5	2.1	2.7	0.78	1.3	-2.9	42	20	10	8.0
5.0	5.0	3.2	1.56	9.0	14.8	45	20	10	8.1
5.6	5.7	3.3	1.73	13.7	21.6	45	20	11	5.5
6.3	5.1	3.0	1.70	10.7	17.0	45	21	11	5.6
6.6	5.4	2.8	1.93	14.1	21.3	48	22	11	6.8
7.3	5.6	2.7	2.07	16.2	24.1	50	22	14	6.5
7.7	5.7	3.3	1.73	13.7	21.6	50	22	12	8.3
8.0	5.4	3.1	1.74	12.4	19.6	50	23	12	5.0
8.3	5.3	2.8	1.89	13.3	20.1	50	24	12	10.7
8.6	5.1	3.1	1.65	10.2	16.4	50	25	14	8.9
8.9	5.0	3.4	1.47	8.0	13.4	50	26	13	-
9.2	5.5	3.5	1.57	11.0	18.0	55	28	15	8.5
9.4	6.5	4.3	1.51	14.3	23.8	60	30	15	13.8
9.8	7.1	4.5	1.58	18.5	30.2	70	40	16	8.2
10.1	7.8	5.2	1.50	20.3	33.8	80	50	18	12.9
10.5	12.5	7.4	1.65	63.8	101.5	85	60	22	15.8
10.6*	13.9	8.1	1.72	80.6	127.6	90	65	29	23.8

* Scored at end of test

APPENDIX C

DISC SCORING TEST SERIES

Load: 4741 N (1066 lbs) to scoring, 2518 N (566 lbs) for 5 minutes after scoring then reload to 4741 N (1066 lbs).

V_A (Tangential Velocity of Lower Roller) = 3.49 m/sec (137.4 ips)

Filter Rating: No filter

Elapsed Time (Hrs.)	R.T. FERROGRAPH					GEOM		SOA	Scoring
	A_L	A_S	SI_1	SI_2	SI_3	Scatter	Attentuation	PPM(Fe)	Event
0.0	-	-	-	-	-	0	-2	1	
0.8	12.9	6.5	1.9	77.4	118.8	23	16		
0.9	21.5	11.8	1.8	208.6	323.0	42	36	20	*
1.4	27.1	13.8	2.0	360.4	544.0	55	40		
1.8									*
2.0	27.1	14.3	1.9	346.9	529.9	55	50	28	
2.4	25.9	13.4	1.9	323.8	491.3	60	55		
3.0	26.9	14.5	1.9	333.6	513.4	70	60		*

FILTRATION SERIES

FILTER RATING (μM)								
75	25.4	14.4	1.8	279.4	437.8			
40	23.8	12.6	1.9	266.6	407.7			
25	24.4	15.2	1.6	224.5	364.3			
10	4.8	4.3	1.1	2.4	4.6	50	41	22

APPENDIX C

DISC SCORING TEST SERIES

Load: 4741 N (1066 lbs) to scoring, 2518 N (566 lbs) for 5 minutes after scoring then reload to 4741 N (1066 lbs).

V_A (Tangential Velocity of Lower Roller) = 3.49 m/sec (137.4 ips)

Filter Rating: 75 Micrometre

Elapsed Time (Hrs.)	R.T. FERROGRAPH A_L	A_S	SI_1	SI_2	SI_3	GEOM Scatter	Attentuation	SOA PPM(Fe)	Scoring Event
0.0	0.7	0.1	7.0	0.4	0.5	20	7	4	
0.4	34.6	19.7	1.8	515.5	809.1	105	85		*
0.6	37.8	21.7	1.7	608.6	958.0	130	110	44	
0.9	39.9	24.3	1.6	622.4	1001.5	140	125		*
1.3	39.1	24.9	1.6	555.2	908.8	155	130	52	*

FILTRATION SERIES

FILTER RATING (μM)									
40	30.6	19.3	1.6	345.8	563.9	145	125	44	
25	25.0	18.3	1.4	167.5	290.1	140	125	45	
10	10.0	8.6	1.2	14.0	26.0	100	90	32	

APPENDIX C

DISC SCORING TEST SERIES

Load: 4741 N (1066 lbs) to scoring, 2518 N (566 lbs) for 5 minutes after scoring then reload to 4741 N (1066 lbs).

V_A (Tangential Velocity of Lower Roller) = 3.49 m/sec (137.4 ips)

Filter Rating: 40 Micrometre

Elapsed Time (Hrs.)	R.T. FERROGRAPH A_L	A_S	SI_1	SI_2	SI_3	GEOM Scatter	GEOM Attentuation	SOA PPM(Fe)	Scoring Event
0.0	0.3	-0.7	-0.4	0.3	-0.4	10	5	5	
0.7	22.5	16.0	1.4	146.3	250.3	55	42	29	*
1.7	24.3	18.2	1.3	148.2	259.3	80	65	46	
1.9									*
2.1	24.7	19.1	1.3	138.3	245.3	85	65		
2.7	22.8	17.3	1.3	125.4	220.6	85	70	45	
3.0	21.9	16.8	1.3	111.7	197.4	85	70		
3.3	21.6	16.3	1.3	114.5	200.9	80	70		
3.8	19.6	15.3	1.3	84.3	150.1	85	65		
4.4	19.0	15.0	1.3	76.0	136.0	85	75	44	*

FILTRATION SERIES

FILTER RATING (μM)									
25	19.0	15.0	1.3	76.0	136.0	80	65	48	
10	10.8	9.8	1.1	10.8	20.6	85	70	45	

APPENDIX C

DISC SCORING TEST SERIES

Load: 4741 N (1066 lbs) to scoring, 2518 N (566 lbs) for 5 minutes after scoring then reload to 4741 N (1066 lbs).

V_A (Tangential Velocity of Lower Roller) = 3.49 m/sec (137.4 ips)

Filter Rating: 25 Micrometre

Elapsed Time (Hrs.)	R.T. FERROGRAPH					GEOM		SOA	Scoring Event
	A_L	A_S	SI_1	SI_2	SI_3	Scatter	Attentuation	PPM(Fe)	
0.0	3.0	1.1	2.7	5.7	7.8	20	7	5	
0.6	4.2	3.0	1.4	5.0	8.6	22	10		
0.9	3.9	3.2	1.2	2.7	5.0	22	10	6	
1.4	4.5	4.0	1.1	2.3	4.3	25	14	8	*
1.5									*
1.8	7.8	5.3	1.5	19.5	32.8	29	17	10	
2.3	7.9	6.3	1.3	12.6	22.7	35	20		
2.3	8.6	6.9	1.3	14.6	26.4	32	22	11	*

FILTRATION SERIES

FILTER RATING (μM)									
10	4.9	4.2	1.2	3.4	6.4	30	20	12	

APPENDIX C

DISC SCORING TEST SERIES

Load: 4741 N (1066 lbs) to scoring, 2518 N (566 lbs) for 5 minutes after scoring then reload to 4741 N (1066 lbs).

V_A (Tangential Velocity of Lower Roller) = 3.49 m/sec (137.4 ips)

Filter Rating: 10 Micrometre

Elapsed Time (Hrs.)	R.T. FERROGRAPH					GEOM		SOA	Scoring Event
	A_L	A_S	SI_1	SI_2	SI_3	Scatter	Attentuation	PPM(Fe)	
0.0	-1.0	-1.2	0.8	+0.2	-0.4	4	0	1	
0.6	6.6	5.5	1.2	7.3	13.3	35	25		*
0.6	7.6	6.5	1.2	8.4	15.5	33	24	13	
1.3	9.1	7.6	1.2	13.7	25.1	34	25	16	*
1.6	9.9	8.2	1.2	16.8	30.8	37	23		
1.6	8.9	7.2	1.2	15.1	27.4	26	20	16	*

APPENDIX D

BEARING TEST SERIES

Load: 18085 N (4066 lbs) Prior to fatigue spall
4741 N (566 lbs) After spall

Speed: 549.8 rps (5250 rpm)

Filter Rating: No Filter

Elapsed Time (Hrs.)	R.T. FERROGRAPH A_L	A_S	SI_1	SI_2	SI_3	GEOM Scatter	Attentuation	SOA PPM(Fe)	UTRC X-RAY
0.0	3.3	1.4	2.4	6.3	8.9	3	0	1	0.0
0.2	61.2	32.0	1.9	1787.0	2721.4	95	65	29	37.8
0.5	68.0	40.0	1.7	1904.0	3024.0	100	85	29	46.5

FILTRATION SERIES

FILTER RATING (μM)									
75	55.0	33.1	1.7	1204.5	1929.4	125	100	26	23.3
40	52.8	31.6	1.7	1119.4	1789.3	125	100	23	22.6
25	19.4	13.3	1.5	118.3	199.5	100	60	14	6.2
10	9.4	6.6	1.4	26.3	44.8	65	38	9	10.5

Note: No spalling occurred. Failure resulted from excessive cage wear.

APPENDIX D

BEARING TEST SERIES

Load: 18085 N (4066 lbs) Prior to fatigue spall
4741 N (566 lbs) After spall

Speed: 549.8 rps (5250 rpm)

Filter Rating: 75 Micrometre

Elapsed Time (Hrs.)	R.T. FERROGRAPH A_L	A_S	SI_1	SI_2	SI_3	GEOM Scatter	GEOM Attentuation	SOA PPM(Fe)
0.0	-0.3	0.2	-1.5	0.15	0.05	0	0	1
0.5	10.6	3.7	2.9	73.1	98.7	17	7	
0.9	22.2	8.9	2.5	295.3	413.6	22	10	6
1.4	30.7	10.7	2.9	614.0	828.0	27	14	
2.1	36.3	12.5	2.9	863.9	1161.4	26	16	9
2.4	37.0	12.8	2.9	895.4	1205.2	32	16	
3.1	18.0	8.0	2.3	180.0	260.0	28	16	9
3.4	24.2	10.6	2.3	329.1	473.3	33	18	
4.0	27.9	12.3	2.3	435.2	627.1	36	20	7
4.7*	32.1	12.4	2.6	632.4	876.7	45	25	
4.7	32.4	13.8	2.4	602.6	859.3	50	28	15
5.1	24.6	10.8	2.3	339.5	488.5	28	16	13
5.6	40.7	21.4	1.9	785.5	1198.5	34	22	17
6.0	51.1	24.8	2.1	1343.9	1996.2	37	20	
6.5	54.1	26.6	2.0	1487.8	2219.3	39	23	19
7.0	52.1	26.3	2.0	1344.2	2022.7	43	26	
7.5	52.1	26.7	2.0	1323.3	2001.5	45	28	20
8.0	49.5	25.7	1.9	1178.1	1789.8	45	28	
8.6	46.6	25.8	1.8	969.3	1505.9	55	33	28

FILTRATION SERIES

FILTER RATING (μM)								
40	36.5	21.0	1.7	565.8	891.3	50	34	25
25	31.0	19.6	1.6	353.4	576.8	55	33	24
10	12.7	8.4	1.5	54.6	90.7	44	28	10

*Bearing initial fatigue spall

APPENDIX D

BEARING TEST SERIES

Load: 18085 N (4066 lbs) Prior to fatigue spall
4741 N (566 lbs) After spall

Speed: 549.8 rps (5250 rpm)

Filter Rating: 40 Micrometre

Elapsed Time (Hrs.)	R.T. FERROGRAPH					GEOM		SOA
	A_L	A_S	SI_1	SI_2	SI_3	Scatter	Attentuation	PPM(Fe)
0.0	0.0	0.0	-	0.0	0.0	7	1	3
1.5*	12.7	6.5	2.0	78.7	119.0	13	7	5
2.3	7.7	3.6	2.1	31.6	46.3	16	7	5
2.9	6.8	4.1	1.7	18.4	29.4	13	8	4
3.8	5.0	3.1	1.6	9.5	15.4	14	9	5
4.9	5.0	2.3	2.2	13.5	19.7	15	10	6
5.9	4.6	2.3	2.0	10.6	15.9	16	10	6
6.6	8.0	4.4	1.8	28.8	44.6	21	15	8
7.6	11.1	6.1	1.8	55.5	86.0	32	21	8
8.5	8.4	5.1	1.7	27.7	44.6	29	21	8
9.5	10.0	5.6	1.8	44.0	68.6	35	24	9
10.2	20.5	8.6	2.4	244.0	346.3	39	23	11
FILTER BY-PASS								
11.1	20.0	8.6	2.3	228.0	326.0	60	36	16
12.0	16.5	8.6	1.9	130.4	198.3	65	41	17
12.6	9.0	4.0	2.3	45.0	65.0	50	30	3
13.6	13.7	6.6	2.1	97.3	144.1	60	36	12
14.3	11.2	7.0	1.6	47.0	76.4	70	39	14

FILTRATION SERIES

FILTER RATING (μM)								
40	18.0	9.5	1.9	153.0	233.8	75	44	14
10	5.0	4.3	1.2	3.5	6.5	65	40	16

*Bearing initial fatigue spall

APPENDIX D

BEARING TEST SERIES

Load: 18085 N (4066 lbs) Prior to fatigue spall
4741 N (566 lbs) After spall

Speed: 549.8 rps (5250 rpm)

Filter Rating: 25 Micrometre

Elapsed Time (Hrs.)	R.T. FERROGRAPH					GEOM		SOA	SOA
	A_L	A_S	SI_1	SI_2	SI_3	Scatter	Attentuation	PPM(Fe) (1)	PPM(Fe) (2)
0.1	2.4	1.7	1.4	1.7	2.9	20	8	4	4
0.8	7.3	4.6	1.6	19.7	32.1	22	11	-	-
1.9*	3.0	2.5	1.2	1.5	2.8	42	20	1	7
1.9	4.2	1.3	3.2	12.2	16.0	42	20	8	5
2.1	5.3	3.0	1.8	12.2	19.1	50	25	-	8
2.9	4.8	3.7	1.3	5.3	9.4	55	28	12	9
3.6	11.5	7.6	1.5	44.9	74.5	90	55	10	16

FILTRATION SERIES

FILTER RATING (μM)									
10	7.4	3.7	2.0	27.3	41.1	45	26	21	8

*Bearing initial fatigue spall

NOTES: (1) SOA reading "suspect" because the samples were lost and then found after an inquiry.

(2) Duplicate samples submitted.

APPENDIX D

BEARING TEST SERIES

Load: 18085 N (4066 lbs) Prior to fatigue spall
4741 N (566 lbs) After spall

Speed: 549.8 rps (5250 rpm)

Filter Rating: 10 Micrometre

Elapsed Time (Hrs.)	R.T. FERROGRAPH					GEOM		SOA
	A_L	A_S	SI_1	SI_2	SI_3	Scatter	Attentuation	PPM(Fe)
0.0	-0.3	-0.4	0.75	0.30	-0.07	5	4	2
0.7	0.9	0.9	1.00	0.00	0.00	7	6	
1.0	1.8	1.1	1.60	1.30	2.00	6	5	2
1.7	1.2	1.0	1.20	0.24	0.44	4	4	
2.2	1.1	1.2	0.92	0.11	-0.23	4	3	2
2.7	-0.3	0.1	-3.00	0.12	0.08	3	2	
3.2	0.2	0.3	0.66	-0.02	-0.05	3	3	2
3.7	0.4	0.3	1.33	0.04	0.07	3	3	
4.0	-0.2	0.3	-0.66	0.10	-0.05	3	3	2
4.4*	0.2	-1.2	-0.16	0.28	-1.40	4	4	2
4.9	0.3	-0.8	-0.40	0.33	-0.60	3	3	
5.4	-0.1	0.2	-0.50	0.03	-0.03	3	3	2
5.9	-0.4	0.3	-1.33	0.28	0.07	3	3	
6.2	0.5	0.4	1.25	0.05	0.09	2	2	2
6.7	-	-	-	-	-	3	4	
7.2	0.5	0.4	1.25	0.05	0.09	3	3	2
7.7	0.1	-0.4	-0.25	0.05	-0.15	5	2	
8.2	-0.1	0.4	-0.25	0.05	-0.15	1	3	1
8.8	-1.0	-0.7	1.40	0.30	0.51	7	6	3
9.3	0.2	0.4	0.50	-0.04	-0.12	3	3	
9.8	0.3	0.7	0.43	0.12	-0.40	1	2	2
10.3	0.2	-0.8	-0.25	0.20	-0.60	1	2	
10.8	-0.5	0.1	-5.00	0.30	0.24	2	2	2
11.3	0.3	0.4	0.75	0.03	-0.07	3	2	
11.8	-0.3	0.2	-1.50	0.15	0.05	3	2	2
12.3	-0.2	0.1	-2.00	0.06	0.03	2	2	
12.8	-0.1	0.2	-0.50	0.03	-0.03	2	2	2

* Bearing initial fatigue spall.

DISTRIBUTION LIST

	COPIES
Naval Air Systems Command (AIR-50174), Department of the Navy, Washington, DC 20361	14

Intra-Command Addressees

AIR-50174	(2)	AIR-52032	(1)
AIR-06	(1)	AIR-52031	(1)
AIR-536	(1)	AIR-330	(1)
AIR-5364	(1)	AIR-330A	(1)
AIR-5364C	(1)	AIR-310	(1)
AIR-53645	(1)	AIR-340E	(1)
		AIR-320A	(1)

Chief of Naval Material, (Code MAT 08T242 LCDR T.Hinton) Washington, DC 20360	1
Commander, Naval Air Development Center, (Code 30212 N. Rebuck & L. Stallings) Warminster, Pa. 18974	2
Commanding Officer, Naval Research Laboratory, (Code 6170 H. Ravner), Department of the Navy, Washington, DC 20375	1
Chief of Naval Research (Code 473 - R.S. Miller), Arlington, VA 22217	1
Commander, Naval Air Engineering Center, Naval Air Station Lakehurst, (Code 92724 P.B.Senholzi), Lakehurst, N.J. 08733	1
Commanding Officer, Naval Air Rework Facility, Naval Air Station Pensacola, (Code 360 R.B.Kight, J.C.Jennings & R.S. Lee), Pensacola, Florida 32508	3
Commanding Officer, Naval Air Rework Facility, Naval Air Station North Island (Code 341 D. Stanley), San Diego, Cal. 92135	1
Commander, Naval Air Test Center, Engineering Services Section, Systems Engineering Test Directorate, (Code SY-42 L.A.Mileto and T.A.Bowles), Patuxent River, MD 20670	2
Superintendent, Naval Postgraduate School, Monterey, CA 93940	1
Commander, Naval Ship Engineering Center, (Code 6107 D.C. Metcalf & G.F.Rester), Washington DC 20362	2

NAPC-PE-2

	COPIES
Commander, David W. Taylor Naval Ship Research and Development Center, (Code 2832 N. Glassman and D.L. Craven, Code 2831 R.W.McQuaid), Annapolis, MD 21402	3
Commander, Air Force Aero Propulsion Laboratory,(Code AFAPL/SFL H. Jones), Wright Patterson AFB, Ohio 45433	1
Commander, Air Force Materials Laboratory, (Code AFML/LNL R. Benzing), Wright Patterson AFB, Ohio 45433	1
Commanding Officer, U.S. Army Aviation Systems Command, (Aircraft Power Plants Branch) (Code DRSAD-LEP S. Chen), 12th and Spruce Sts., St. Louis, MO 63166	1
Director, Applied Technology Laboratory, U.S. Army Research and Technology Laboratories (AVRADCOM) (Codes DADL-E-MOR D. Lubrano and DADL-E-TAP D. Pauze) Ft. Eustis, VA 23604	2
Director, U.S. Army Ballistic Research Laboratories, (Code AMXBR-VL/W.Thompson), Aberdeen Proving Ground, MD 21005	1
Director, U.S. Army Air Mobility R&D Lab-Lewis, (Code MS-77-5 E. Bailey), 2100 Brookpark Rd., Cleveland, Ohio 44135	1
Administrator, NASA-Lewis Research Center, (Code MS-23-2 W. Jones), 2100 Brookpark Rd., Cleveland, Ohio 44135	1
Defense Documentation Center for Scientific and Technical Information (DDC), Building No. 5, Cameron Station, Alexandria, Virginia 22314	12
Pratt and Whitney Aircraft Group, Government Products Division, West Palm Beach, Florida 33402, Attn: John Miner	1
Pratt and Whitney Aircraft, Commercial Products Division, 400 Main Street, EBZG3, E. Hartford, Conn. 06108 Attn: P.T.George	1
United Technologies Research Center, Silver Lane, E. Hartford, Conn. 06108 Attn: L.L.Packer	1
General Electric Co., 50 Fordham Rd., Wilmington Mass. 01887 Attn: C.E. Buzzell	1
General Electric Co., 1000 Western Ave., T700 System Engineering, Lynn Mass 01910, Attn: G.P.Sirois, IMZ 24010	1
General Electric Co., 1000 Western Ave., T700 C & A Design, Lynn Mass. 01910 Attn: M.M.Rosen IMZ 24002	1

	COPIES
General Electric Co., 1000 Western Ave., Product Assurance and Diagnostics, Lynn, Mass. 01910, Attn: H.J.Jordan, IMZ 24056	1
Baird-Atomic, 125 Middlesex Turnpike, Bedford, Mass. 01730, Attn: D.V.Dunn and J.F.McCadden	2
Oklahoma State University, Fluid Power Research Center, Stillwater, Oklahoma 74074, Attn: R.K.Tessman and G.E.Maroney	2
Foxboro/Trans-Sonics, Inc., P.O. Box 435, Burlington, Mass 01803, Attn: E.R.Bowen and V.C.Wescott	2
Environment One Corp., 2773 Balltown Rd., Schnectady, N.Y. 12309, Attn: E. DeMetre and G.F.Skala	2
Technical Development Co., 24 E. Glenolden Ave., Glenolden, Pa. 19036, Attn: T. Tauber and D. Nielsen	2
Technology/Scientific Services, Inc., Dayton, Ohio 45401, Attn: K. Scheller	1
Michigan Technological University, Mechanical Engineering and Engineering Mechanics Dept., Houghton, MI 49931, Attn: J.H.Johnson	1
Pall Corporation, 30 Sea Cliff Ave., Glen Cove, N.Y. 11542, Attn: W. Needleman	1
Caterpillar Tractor Co., Technical Center, Building E, Peoria, Ill. 61629 Attn: J.M.Perez	1
Exxon Research and Engineering Co., Government Research Laboratory, P.O. Box 51, Linden, N.J. 07036, Attn: A. Beerbower	1
SKF Industries, Inc., 1100 First Ave., King of Prussia, Pa. 19406, Attn: L.B.Sibley	1
Mechanical Technology, Inc. 968 Albany Shaker Rd., Latham, N.Y. 12210, Attn: D.F.Wilcock	1
Shaker Research Corp., Northway 10 Executive Park, Ballston Lake, N.Y. 12019, Attn: J.M.McGrew	1